De-novo purine biosynthesis is a major driver of chemoresistance in glioblastoma

(Supplementary materials)

Jack M Shireman, Fatemeh Atashi, Gina Lee, Eunus S. Ali[1], Miranda R. Saathoff, Cheol H. Park, Sol Savchuk, Shivani Baisiwala, Jason Miska, Maciej S. Lesniak, C. David James, Roger Stupp, Priya Kumthekar, Craig M. Horbinski, Issam Ben-Sahra[1], and Atique U. Ahmed*

One Sentence Summary: *De-novo* purine biosynthesis, which promotes chemoresistance in GBM, can be disrupted by FDA approved Mycophenolate Mofetil improving therapeutic outcomes.

Department of Neurological Surgery, [1]Department of Biochemistry and Molecular Genetics, Feinberg School of Medicine, Northwestern University, Chicago, IL USA 60616

Supplementary Figure Legends:

Supplementary Figure 1: Chemical and shRNA inhibition of EZH2 impairs maintenance of BTIC niche. **A/B**: FACS plots showing percent EZH2+, CD133+, and EZH2+/CD133+ double positive populations of cells in response to TMZ therapy across two GBM cells lines. Bar graphs representing single positive populations as percent of parent (live cells). Error bars represent technical triplicates. **C**: Bar graphs representing percent of corresponding positive cells in the FACS analysis of flank GBM43 tumors. Far Left. FACS plots showing percent CD133+, CD15+, and CD133+/CD15+ double positive populations following treatment with DZNep with and without TMZ. Bar graphs representing single positive populations of known BTIC compartment markers as percent of parent (live cells). *** p<.001. **D.** Extreme limiting dilution analysis assay on cells with shRNA KD of HIF1A compared to nontargeted guide RNA. Error bars demonstrate 95% CI of stem cell frequency p-value determined from 12-well replicates of plate counting in provided software. Bottom, bar graph representing the number of tumorsphere in each well.

Supplementary Figure 2: HIF1A expression is correlated with EZH2 levels in patient data. **A**: Bar graphs displaying Mean Fluorescent Intensity (MFI) of shRNA mediated KD cells stained for HIF1A and HIF2A. **p<.01 ***p<.001. **B**: GlioVis data visualization and analysis platform showing relationship between EZH2 and HIF1A gathered from the Chinese Glioma Genome Atlas ($r=0.4$, $p < 0.005$) and Rembrandt ($r=0.52$, $p < 0.005$) datasets respectively. **C**: Gene expression Jitterplots showing relative transcript levels of HIF1A and EZH2 stratified by cell type. Confidence interval plots representing results of Tukey's Pairwise Comparison for HIF1A and EZH2.

Supplementary Figure 3: Top 5 EZH2 targets during Temozolomide therapy. GBM43 and GBM6 were treated with either vehicle control or DZNep (0.05 nM) in combination with TMZ

(50μM) for 48 hours. Gene expression analysis between the different subtypes of GBM identified *ARL13B* as one of the top genes for which expression was altered in the absence of EZH2 activity (fold change >3, $p<0.05$). Top 5 genes identified from these experiments next evaluated for clinical significance in GBM patients sample by using GlioVis. The mRNA expression (log 2, p-values Bonferroni correction) in different histological grades of brain tumor as well as patients overall survival based on high and low (cutoff: median) expression are analyzed.

Supplementary Figure 4: Binding of EZH2 across DNA, as well as global gene expression, is altered during TMZ therapy. **A**: Annotated VennPie plot generated from ChIPSeeker expressing distribution of EZH2 binding locations during TMZ therapy called over input DNA control. **B**: Microarray data examining global gene expression after 4 days and 8 days post TMZ therapy. **C**: ChIP data profiling H3K27ac at transcription start sites of genes found with significant alterations in expression patterns in microarray data. Yellow highlights represent statistically significant peaks post TMZ treatment that fall within the transcription start site of the genes assayed. Table indicates peak location and fold enrichment over DMSO control. String analyses of microarray targets that were also shown to have increased H3K27ac at transcription start site during TMZ therapy. **D**: Western bots profiling protein levels of these targets in GBM43 (proneural) and GBM5 (mesenchymal) cell lines. **E**: Table of multiple ChIP assays performed examining binding events within an identified ARL13B enhancer site as well as the transcription start site of ARL13B. Significance determined by BED file statistics reported from macs2 **F**: Western blot images showing expression levels of EZH2 and ARL13B under EZH2 shRNA-mediated knockdown and TMZ conditions Day 1 and 2 post therapy.

Supplementary Figure 5: ARL13B expression is related to EZH2 levels and is correlated in both primary and recurrent tumors. **A**: CGGA data comparing expression of ARL13B and EZH2 in primary GBM **B**: CGGA data comparing expression of ARL13B and IMPDH2 in recurrent GBM. **C**: Immunohistochemistry (IHC) images of matched primary and recurrent patient samples stained for ARL13B. *n*=8.

Supplementary Figure 6: ARL13B promotes stemness in PDX GBM. **A.** Number of tumorsphere in each well of ARL13B knockdown and rescue experiments in Figure 3B extreme limiting dilution analysis assay. **B.** Cells cultured under stem cell conditions have increased levels of ARL13B. Western blot images comparing expression levels of several proteins in cells raised in stem cell (supplemented Neurobasil media) versus differentiated (serum grown) conditions. Data representing in vitro cultures of three different PDX lines GBM5 (mesenchymal) GBM6 (classical) GBM43 (proneural).

Supplementary Figure 7: Expression of known downstream targets of ARL13B is unaltered in response to several anti-GBM treatments. **A**: Immunofluorescence (IF) analysis of ARL13B positive cilia structure in PDX GBM43 with Sonic Hedgehog signaling molecules SMO and GLI1. **B:** IF analysis of ARL13B positive cilia structure in PDX GBM43 co-staining with AC-tubulin. **C:** IFimages of in vitro PDX cells probed with anti-ARL13B (green) and DAPI (blue). Ciliary structures indicated by white arrows. Bar graph representing length of cilia assessed at multiple points over eight days of treatment compared to vehicle control. **D:** In vivo IF analysis of PDX GBM43 without therapy (DMSO), during therapy (TMZ primary) and post therapy recurrent (TMZ recurrent) GBM xenograft demonstrating the presence of ARL13B cilia. Below, the bar graph demonstrating the cilia number decrease during therapy but significantly increased in recurrent GBM (n=3). ***p<.001, **p<.01. **E**: Western blot images displaying expression of

various downstream targets of ARL13B following the indicated treatments across GBM6 and GBM52 cell lines.

Supplementary Figure 8: ARL13B and EZH2 expression correlate with Cilia formation but pharmacological loss of cilia does not improve response to TMZ chemotherapy. **A**: IF showing in vitro cultured cells stained with DAPI (blue), ARL13B (red), and ARL13B in knockdown condition (Green). Cells from both conditions were treated with DMSO or TMZ. **B**: IF of in vitro cultured PDX cells stained with DAPI (blue), ARL13B (green), and EZH2 (purple). Regions expressing high or low amounts of EZH2 as indicated by fluorescence intensity were isolated and quantified. Column graph visualizing number of cilia within a microscope field of view if cells have either high or low expression of EZH2 n=7 separate fields. **C**: MTT assay survival graph performed on GBM 43 pdx cells treated with varying doses of a pharmacological disruptor of cilia (Ciliobrevin) either alone or in combination with TMZ. Error bars depict technical replicates among experiments. ****p<.0001

Supplementary Figure 9: ARL13B and EZH2 protein levels increase post TMZ therapy and ARL13B and IMPDH2 interaction is also seen in breast cancer cells as well as multiple PDX subtypes. **A/B**: Western blots performed after exposure to therapy or vehicle control on GBM6 (classical) and GBM 43 (proneural). **C**: IP of ARL13B performed on cultured breast cancer cell lines probing for ARL13B and IMPDH2 interaction. **D**: IP of ARL13B performed on cultured PDX lines GBM6 (classical) and GBM43 (proneural) treated with DMSO or TMZ probing for ARL13B and IMPDH2 interaction as well as interaction with ciliary protein IF43.

Supplementary Figure 10: QPCR and ChipSeq demonstrate purine biosynthesis enzymes are altered post TMZ therapy. QPCR data collected on GBM 43 (proneural) across DMSO or TMZ treatment for 2 days or 4 days probing common purine biosynthetic genes. ChIPSeq demonstrated transcription start site enrichment of H3K27ac was also present. Fold enrichment and p value statistics calculated by macs2 and compared to DMSO vehicle control enrichment. Yellow highlights indicate peak within transcription start site.

Supplementary Figure 11: Purine turnover in the liver as well as PDX tumors grown subcutaneously in a flank show response to TMZ treatment. **A**: Graphs of total ion counts of isolated tissues from mouse brain as well as liver after mice had received either TMZ or DMSO treatment prior to hypoxanthine infusion. **B**: Fractional enrichment of IMP+5 and GMP+5 compared to Hypoxanthine +5 in the liver of mice treated with either DMSO or TMZ. **C**: Fractional enrichment of IMP+5 and GMP+5 compared to Hypoxanthine +5 in a single mouse where a GBM43 tumor was isolated from the brain as well as isolated from the subcutaneous flank and normal brain tissue.

Supplementary Figure 12: Steady state metabolic profiling of control and ARL13B knockout cells indicates altered purine biosynthesis after loss of ARl13B. Metabolites from Figure 5 in vivo tracing were assayed using cells with normal levels of ARL13B or lacking ARL13B because of CRISPR deletion. Cells were also treated with DMSO or TMZ. Error bars indicate SD of technical replicates n=3.

Supplementary Figure 13: Expression of purine transporters is altered in response to TMZ and BCNU causes similar effects to TMZ with respect to DNA damage. **A**: Gene expression data from microarray analysis showing levels of several equilibrative and concentrative nucleoside transporters. **B**: Cells with or without ARL13B were treated with vehicle control or BCNU. Representative images of staining are displayed. Graph indicates blinded experimenter foci counts n=30 cells counted. **** p<.0001 2-wayANOVA adjusted for multiple comparisons.

Supplementary Figure 14: MMF causes increased DNA damage during combinatory treatment with TMZ but can be overcome with ARL13B overexpression. **A**: Representative images showing treatment with MMF (cellcept) at 50um combined with TMZ (50um) in the brightfield (live dead) and fluorescent (pH2ax) channels. **B**: In vitro survival assays done with MTT showing percent live cells in GBM 43 (proneural) and GBM6 (mesenchymal) treated with varying doses of MMF alone or in combination with 50um TMZ. **C**: Western blot in virally overexpressed U251 cells probing ARL13B protein levels across samples lacking ARL13B endogenously but infected with 1 infection unit of rescue virus or 20 infection units of rescue virus. **D**: MTT showing percent live cells treated over a TMZ dosing range from 0-500um in cells that contained normal ARL13B levels, reduced ARl13B levels, as well as rescued ARL13B overexpression. **E**: MTT assay showing percent live cells across TMZ treatments ranging from 0-500um combined with 5um MMF in cells with WT ARL13B expression, Loss of ARL13B, rescue of ARL13B expression, and rescue overexpression of ARL13B.

Supplementary Figure 15: In vivo efficacy of differing doses of Mycophenolate Mofetil. **A**: Kaplan-Meier Curve representing results of experiment comparing the anti-tumor efficacy of combination MMF + TMZ versus Mizoribine+ TMZ. Median survival is indicated n=4 mice.

Supplementary Figure 16: MMF+TMZ dosing is no more immune suppressive or toxic in mice than single agent dosing. **A.** Mice were dosed with either MMF alone (150um), TMZ alone (50um), or combination after which FACS separation of T-Regs, Effector CD4's, and CD+ T-Cells was conducted. Data demonstrate that in the brain although there is marked immunosuppression it is not significantly more impacted by the combinatory agent as opposed to the single agents alone. In the spleen, combination treatment did reduce T-Regs, Effector CD4's, and CD+ T-Cell counts but not more than MMF dosing alone. **B**. After a full course (5 days) of the treatments described above were completed blood was collected from mice and sent for analysis of common liver enzymes as well as a complete blood count. Data demonstrates no significant differences in liver enzyme levels or complete blood count measurements between any of the dosing conditions.

Supplementary and Methods:

CRISPR knockout of U251 cells was created by direct transfection with Cas9 nuclease and sgRNA targeting ARL13B (Dharmacon). All cells were passaged by washing one time with phosphate-buffered saline solution (PBS; Gibco) and detached using 0.25% trypsin/2.21mM EDTA (Corning).

***Immunofluorescence*:** For frozen, OCT-embedded (Sakura) tissue, sections were thawed in a 37°C humid chamber for 20 minutes and fixed in 4% paraformaldehyde (PFA; Thermo) for 15 minutes at room temperature. For adherent cells, 8-well chamber slides were taken from 37°C incubators following completion of treatments and fixed 4% PFA for 10 minutes at room temperature. Following fixation, slides were washed two times in 0.05% Tween/PBS solution (PBS-T, Fischer Bioreagents) for 5 minutes and blocked in 10% BSA/0.3% Triton-X/PBS solution at room temperature for 2 hours. Samples were incubated overnight at 4°C in primary antibody mixtures (HIF1α, Biolegend; EZH2, BD Bioscience; ARL13B, ProteinTech; IMPDH2, Abcam; SMO, Santa Cruz; and Gli1, R&D Systems) diluted with 1% BSA/0.3% Triton-X/PBS solution. For unconjugated primaries, the following morning slides were washed three times and incubated at room temperature for 2 hours in secondary antibody mixtures (Invitrogen). Finally, slides were washed three times and mounted using ProLong™ Gold Antifade reagent with Dapi (Invitrogen). Slides were imaged using a fluorescence microscope (Model DMi8; Leica).

***Mass spectroscopy*:** Samples were run on an SDS-PAGE gel, and a gel band was subject to in-gel digestion. Gel band was washed in 100 mM Ammonium Bicarbonate (AmBic)/Acetonitrile (ACN) and reduced with ten mM dithiothreitol at 50°C for 30 minutes. Cysteines were alkylated

with100 mM iodoacetamide in the dark for 30 minutes at room temperature. Gel band was washed in 100mM AmBic/ACN before adding 600 ng trypsin for overnight incubation at 37°C. The supernatant containing peptides was saved into a new tube. The gel was washed at room temperature for ten minutes with gentle shaking in 50% ACN/5% FA, and the supernatant was saved to peptide solution. Washing was repeated each by 80% ACN/5% FA, and 100% ACN, and all supernatant was saved into a peptide solution then subject to speed vac drying. After lyophilization, peptides were reconstituted with 5% ACN/0.1% FA in water and injected onto a trap column (150 μm ID X 3cm in-house packed with ReproSil C18, 3 μm) coupled with an analytical column (75 μm ID X 10.5 cm, PicoChip column packed with ReproSil C18, 3 μm) (New Objectives, Inc., Woburn, MA). Samples were separated using a linear gradient of solvent A (0.1% formic acid in water) and solvent B (0.1% formic acid in ACN) over 120 minutes using a Dionex UltiMate 3000 Rapid Separation nanoLC (ThermoFisher Scientific). MS data were obtained on an Orbitrap Elite Mass Spectrometer (Thermo Fisher Scientific Inc, San Jose, CA). Data were analyzed using Mascot (Matrix Science, Boston, MA) v.2.5.1 against the Swiss-Prot Human database (2019), and results were reported at 1% FDR in Scaffold v.4.8.4 (Proteome Software, Portland, OR). For stable isotope (13C5-hypoxanthine) labeling experiments, dried pellets were resuspended using 20 ul LC-MS grade water for mass spectrometry. 10 μL were injected and analyzed using a 5500 QTRAP triple quadrupole mass spectrometer (AB/SCIEX) coupled to a Prominence UFLC HPLC system (Shimadzu) via selected reaction monitoring (SRM) [24]. Some metabolites were targeted in both positive and negative ion modes for a total of 287 SRM transitions using pos/neg polarity switching. ESI voltage was +4900V in positive ion mode and –4500V in negative ion mode. The dwell time was 3 ms per SRM transition, and the total cycle time was 1.55 seconds. Approximately 10-14 data points were acquired per detected metabolite.

Samples were delivered to the MS via normal phase chromatography using a 4.6 mm i.d x 10 cm Amide Xbridge HILIC column (Waters Corp.) at 350 μL/min. Gradients were run starting from 85% buffer B (HPLC grade acetonitrile) to 42% B from 0-5 minutes; 42% B to 0% B from 5-16 minutes; 0% B was held from 16-24 minutes; 0% B to 85% B from 24-25 minutes; 85% B was held for 7 minutes to re-equilibrate the column. Buffer A was comprised of 20 mM ammonium hydroxide/20 mM ammonium acetate (pH=9.0) in 95:5 water: acetonitrile. Peak areas from the total ion current for each metabolite SRM transition were integrated using MultiQuant v2.0 software (AB/SCIEX). For stable isotope labeling experiments, custom SRMs were created for expected 13C incorporation in various forms for targeted LC-MS/MS.

For all extractions, the remaining pellets were resuspended in 8 M Urea /10 mM Tris, pH 8, heated at 60°C degrees for 30 min with shaking, centrifuged, and protein concentration in the supernatant was quantified using Bradford kit. Peak areas of metabolites detected by mass spectrometry were normalized to the median and then normalized to protein concentrations.

***Extreme limiting dilution assay*:** Following trypsinization, cells are diluted to a concentration of 1 cell/uL in neurobasal media supplemented with glutamine, N2 supplement, B27 supplement, EGF, FGF, and 1% Antibiotic Antimycotic mixture (all components of neurobasal media provided by Gibco). Cells are plated in an untreated 96-well tissue culture plate (VWR) at eight different densities (3 cells/well to 200 cells/well) in replicates of 12. Neurosphere formation is assessed seven days after plating. The analysis is done using the R package provided by the Walter+ and Eliza Hall Institute of Medical Research.

***Flow cytometry*:** Flow cytometric analysis was performed on homogenized tumor tissue after HLA-based isolation from murine brains and adherent PDX cells after trypsinization. Cells were washed three times in PBS, incubated in fixation buffer (eBioscience) for 30 minutes, and

permeabilization buffer for 30 minutes at room temperature. Cells were washed and incubated in primary conjugated antibodies (EZH2, BD Bioscience; CD133, Miltenyi; CD15, Biolegend; Sox2, Sino Biological Inc.; HIF1a, Biolegend; HIF2a, Abcam; and ENT1, Abcam) for 30 minutes at room temperature. Cells were washed a final time, resuspended in 0.5% BSA + TritonX (Sigma) FACS buffer, and analyzed using the BD LSRFortessa 6-Laser (BD Biosciences).

***Western blot*:** After trypsinization, PDX cells were lysed using mammalian protein extraction reagent (mPER; Thermo Scientific) buffer, and protein concentration were quantified via Bradford Assay. Protein samples were prepared by combining with reducing SDS (Alfa Aesar) and boiling at 95°C for 10 minutes. Following denaturation, samples were loaded into 10% polyacrylamide gels, transferred to nitrocellulose membrane (Bio-Rad), and blocked in TBS-T/5% milk solution. Membranes were incubated overnight in primary antibodies (EZH2; Cell Signalling; Beta Actin, ProteinTech; ARL13B, ProteinTech; IMPDH2, Abcam; Oct4, Cell Signaling; Sox2, Cell Signaling; Shh, Cell Signaling; Sufu, Cell Signaling; IFT43, ProteinTech; and ENT1, Abcam) at 4°C and for 2 hours at room temperature in HRP-conjugated secondary antibodies (Cell Signaling).

***Immunoprecipitation*:** Following trypsinization, cells were lysed using mPER buffer, and protein concentration were assessed via Bradford Assay. Samples were incubated overnight at 4°C for antibody crosslinking (anti-HA, ProteinTech; Normal Rabbit IgG, Cell Signalling; ARL13B, ProteinTech; and IMPDH2, Abcam) at a dilution of 1:66. The following morning Protein A/G UltraLink Resin (Thermo) was added to each reaction at a dilution of 1:4 and incubated at room temperature for 2 hours. Precipitates were washed three times with 500uL of mPER buffer and pelleted in a tabletop microfuge for 5 minutes at 2500 xg. Antibody-antigen complexes were eluted in 2X, reducing SDS at 55°C for 10 minutes. Finally, the samples were boiled at 95°C for 5 minutes.

***Immunofluorescence*:** For frozen, OCT-embedded (Sakura) tissue, sections were thawed in a 37°C humid chamber for 20 minutes and fixed in 4% paraformaldehyde (PFA; Thermo) for 15 minutes at room temperature. For adherent cells, 8-well chamber slides were taken from 37°C incubators following completion of treatments and fixed 4% PFA for 10 minutes at room temperature. Following fixation, slides were washed two times in 0.05% Tween/PBS solution (PBS-T, Fischer Bioreagents) for 5 minutes and blocked in 10% BSA/0.3% Triton-X/PBS solution at room temperature for 2 hours. Samples were incubated overnight at 4°C in primary antibody mixtures (HIF1α, Biolegend; EZH2, BD Bioscience; ARL13B, ProteinTech; IMPDH2, Abcam; SMO, Santa Cruz; and Gli1, R&D Systems) diluted with 1% BSA/0.3% Triton-X/PBS solution. For unconjugated primaries, the following morning slides were washed three times and incubated at room temperature for 2 hours in secondary antibody mixtures (Invitrogen). Finally, slides were washed three times and mounted using ProLong™ Gold Antifade reagent with Dapi (Invitrogen). Slides were imaged using a fluorescence microscope (Model DMi8; Leica).

***Microarray*:** Following trypsinization, RNA was extracted from cells using the RNeasy Plus Mini Kit (Qiagen). Microarray analysis was performed using 1,000ng of RNA per manufacturer's guidelines (Illumina). HumanHT12 (48,000 probes, RefSeq plus EST) was used for each microarray. All microarrays were performed in triplicate.

Name	Manufacturer	Cat. No.	Source	Antibodypedia Link
ARL13B	Novus	NBP2-15463SS	Rabbit polyclonal antibody	https://www.antibodypedia.com/gene/32073/ARL13B/antibody/1162431/NBP2-15463
ARL13B	Proteintech	17711-1-AP	Rabbit polyclonal antibody	https://www.antibodypedia.com/gene/32073/ARL13B/antibody/156864/17711-1-AP
IMPDH2-Alexa Fluor 647	Abcam	ab200775	Rabbit monoclonal antibody - AF647	
IMPDH2	Proteintech	12948-1-AP	Rabbit polyclonal antibody	https://www.antibodypedia.com/gene/30367/IMPDH2/antibody/153992/12948-1-AP
IMPDH2	Sigma	ST1578-100UG	Mouse monoclonal antibody (1E12-B6)	
EZH2	Cell Signaling Technology	5246	Rabbit polyclonal antibody	https://www.antibodypedia.com/gene/32761/EZH2/antibody/167141/5246
beta-actin	Proteintech	60008-1-Ig	Mouse monoclonal antibody	https://www.antibodypedia.com/gene/3623/ACTB/antibody/158334/60008-1-Ig
H3K27me3	Cell Signaling Technology	9733	Rabbit polyclonal antibody	
H3K27ac	Cell Signaling Technology	8137P	Rabbit polyclonal antibody	
Nestin	Sigma	N5413	Rabbit polyclonal antibody	
Oct4	Cell Signaling Technology	2890S	Rabbit monoclonal antibody (C52G3)	https://www.antibodypedia.com/gene/26854/POU5F1/antibody/106146/2890
Sox2	Cell Signaling Technology	3579S	Rabbit monoclonal antibody (D6D9)	https://www.antibodypedia.com/gene/3488/SOX2/antibody/106649/3579

Flag tag	Proteintech	20543-1-AP	Rabbit polyclonal antibody	
HA tag	Proteintech	51064-2-AP	Rabbit polyclonal antibody	
pH2A.X (Ser139) Gamma H2A	Cell Signaling Technology	2577S	Rabbit polyclonal antibody	
CD133-APC	Miltenyi Biotech	130-112-316	Recombinant human IgG1 (REA816)	https://www.antibodypedia.com/gene/1554/PROM1/antibody/3231133/130-112-316
CD15-PB	Biolegend	394704	Mouse monoclonal antibody	https://www.antibodypedia.com/gene/3496/FUT4/antibody/4630210/394704
HIF1a	Cell Signaling Technology	14179S	Rabbit monoclonal antibody (D6A8)	https://www.antibodypedia.com/gene/84/HIF1A/antibody/2062077/14179
P39 (CDK5R2)	Invitrogen	PA5-17177	Rabbit polyclonal antibody	https://www.antibodypedia.com/gene/34293/CDK5R2/antibody/634913/PA5-17177
Siglec6	R&D	AF2859	Sheep polyclonal antibody	https://www.antibodypedia.com/gene/2300/SIGLEC6/antibody/696041/AF2859
HOXD10	R&D			
PTPRT	R&D		Goat	
SFTPD	R&D			
Shh	Cell Signaling Technology	2207S	Rabbit monoclonal antibody (C9C5)	https://www.antibodypedia.com/gene/4514/SHH/antibody/105612/2207
SUFU	Cell Signaling Technology	2522S	Rabbit monoclonal antibody (C81H7)	https://www.antibodypedia.com/gene/1768/SUFU/antibody/105848/2522
IFT43	Proteintech	24338-1-AP	Rabbit polyclonal antibody	https://www.antibodypedia.com/gene/191/IFT43/antibody/1266934/24338-1-AP
GAPDH	Proteintech	60004-1-Ig	Mouse monoclonal	https://www.antibodypedia.com/gene/3923/GAPDH/antibody/158060/60004-1-Ig

			antibody (1E6D9)	

Supplementary Table 1. Top binding partners of IMPDH2 during temolozolomide therapy was identified by Immunoprecipitation (IP) using anti-IMPDH2 and Mass Spectroscopy analysis. p-values determined by Scaffold proteomics software.

ARL13B Protein Binding Partners (TMZ Condition)	P-Value (Fishers Exact T-Test Bonferroni Correction Applied)
MYH9_HUMAN	0.0001
ML12A_HUMAN	0.0001
IMDH2_HUMAN	0.0001
PARP1_HUMAN	0.0052
DHE3_HUMAN	0.025
MAGD2_HUMAN	0.12
RL27A_HUMAN	0.072
RS8_HUMAN	0.043
MYH10_HUMAN	0.0001
SRRM1_HUMAN	0.12

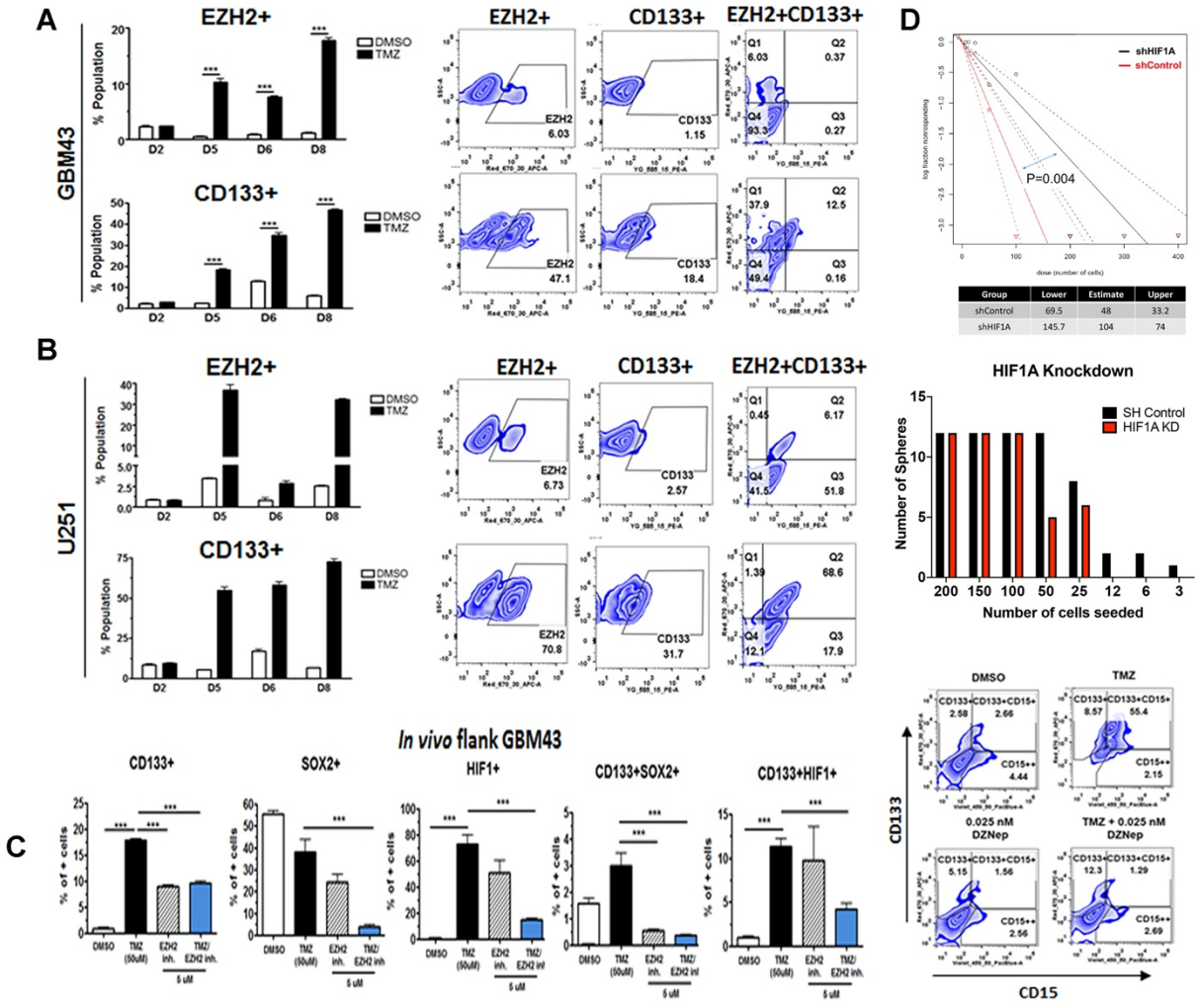
A
GBM43
EZH2+
CD133+
% Population
DMSO
TMZ
D2
D5
D6
D8
EZH2+
CD133+
EZH2+CD133+
EZH2 6.03
CD133 1.15
Q1 6.03
Q2 0.37
Q4 93.3
Q3 0.27
EZH2 47.1
CD133 18.4
Q1 37.9
Q2 12.5
Q4 49.4
Q3 0.16
B
U251
EZH2+
CD133+
% Population
DMSO
TMZ
EZH2+
CD133+
EZH2+CD133+
EZH2 6.73
CD133 2.57
Q1 0.45
Q2 6.17
Q4 41.5
Q3 51.8
EZH2 70.8
CD133 31.7
Q1 1.39
Q2 68.6
Q4 12.1
Q3 17.9
C
In vivo flank GBM43
CD133+
SOX2+
HIF1+
CD133+SOX2+
CD133+HIF1+
% of + cells
DMSO
TMZ (50uM)
EZH2 inh.
TMZ/ EZH2 inh.
5 uM
D
shHIF1A
shControl
P=0.004
log fraction nonsopooning
dose (number of cells)
Group | Lower | Estimate | Upper
shControl | 69.5 | 48 | 33.2
shHIF1A | 145.7 | 104 | 74
HIF1A Knockdown
SH Control
HIF1A KD
Number of Spheres
Number of cells seeded
200 150 100 50 25 12 6 3
DMSO
TMZ
CD133+CD133+CD15+ 2.58 2.66
CD15++ 4.44
CD133+CD133+CD15+ 8.57 55.4
CD15++ 2.15
0.025 nM DZNep
TMZ + 0.025 nM DZNep
CD133+CD133+CD15+ 5.15 1.56
CD15++ 2.56
CD133+CD133+CD15+ 12.3 1.29
CD15++ 2.69
CD133
CD15

Supplementary Figure 2

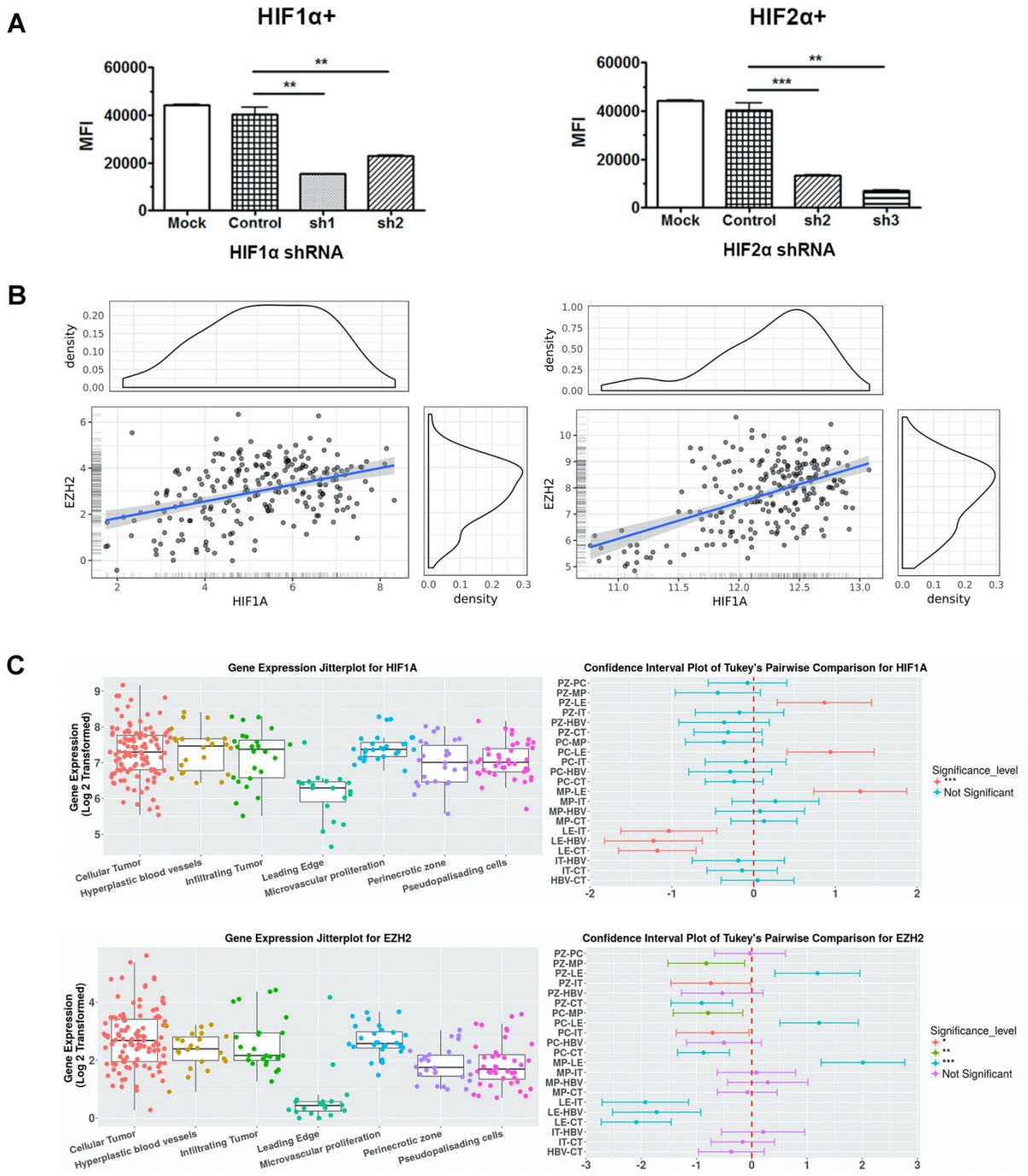

Supplementary Figure 3

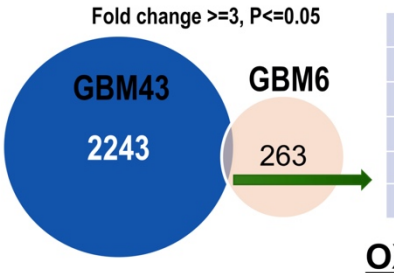

Obs	PROBE ID	Gene Symbol
1	ILMN_1709091	OXGR1
2	ILMN_1748970	PRR15L
3	ILMN_1777301	ARL13B
4	ILMN_3251100	MEF2A
5	ILMN_3294652	TMSB4X

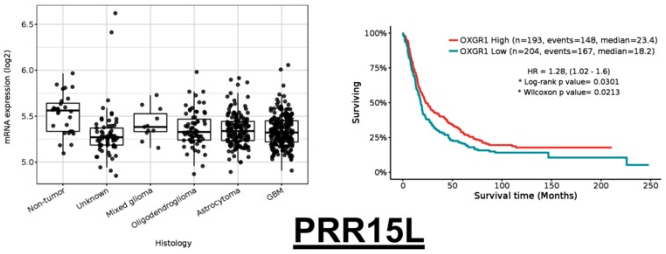

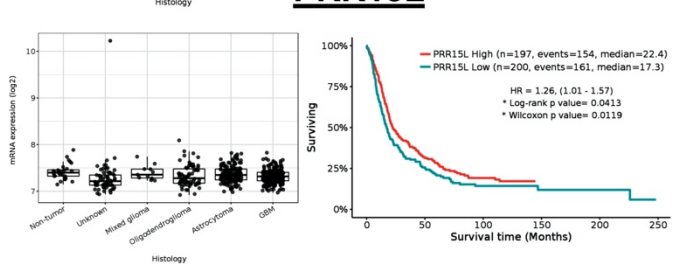

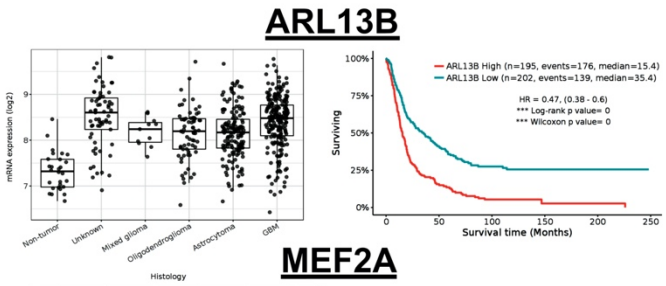

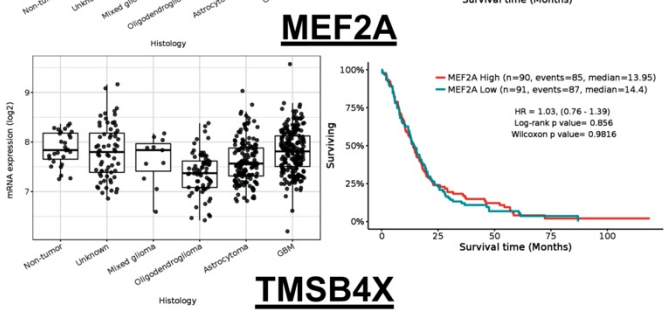

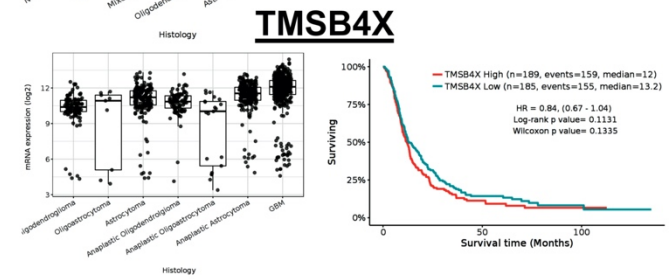

Supplementary Figure 4

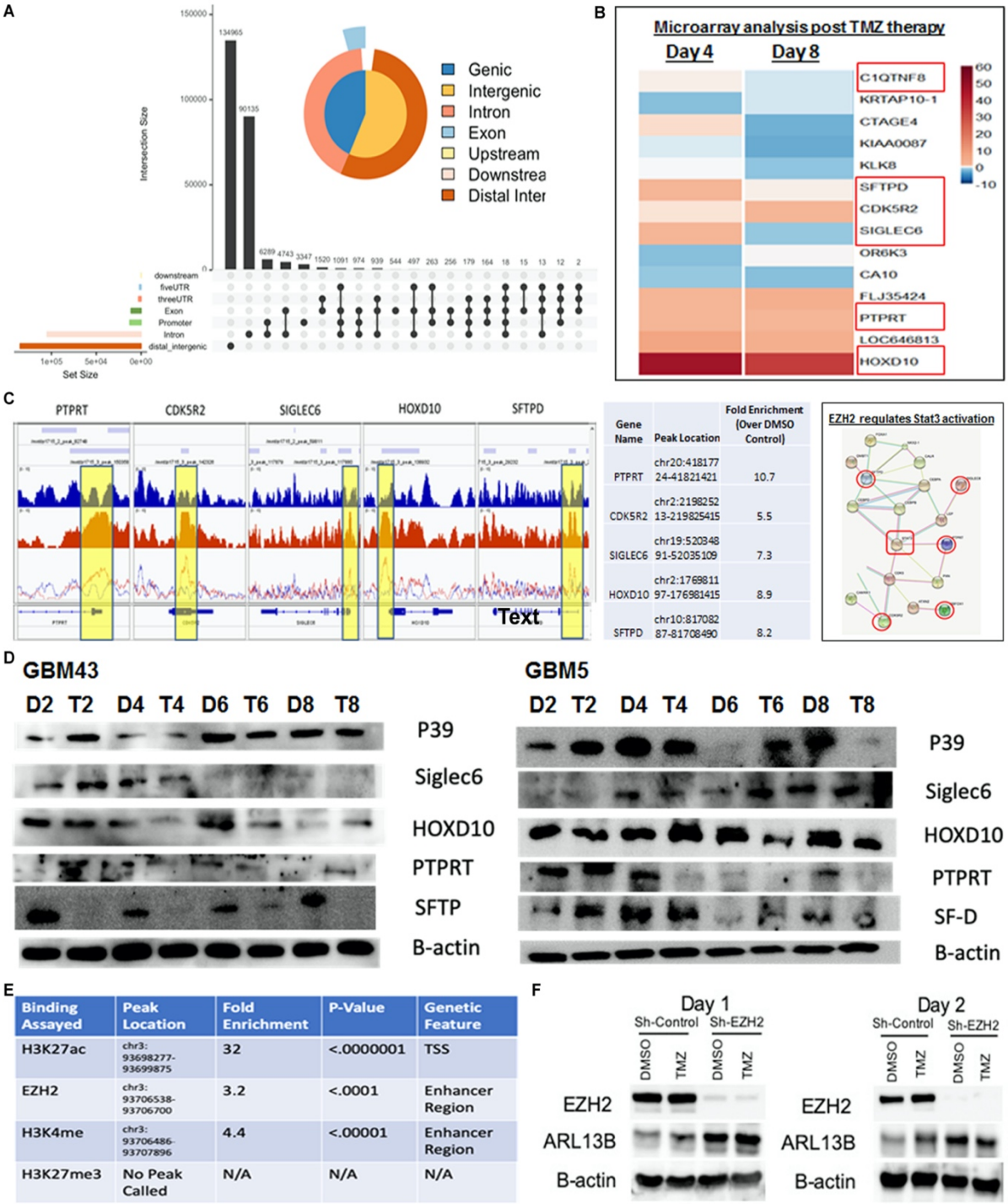

Binding Assayed	Peak Location	Fold Enrichment	P-Value	Genetic Feature
H3K27ac	chr3: 93698277-93699875	32	<.0000001	TSS
EZH2	chr3: 93706538-93706700	3.2	<.0001	Enhancer Region
H3K4me	chr3: 93706486-93707896	4.4	<.00001	Enhancer Region
H3K27me3	No Peak Called	N/A	N/A	N/A

Supplementary Figure 5

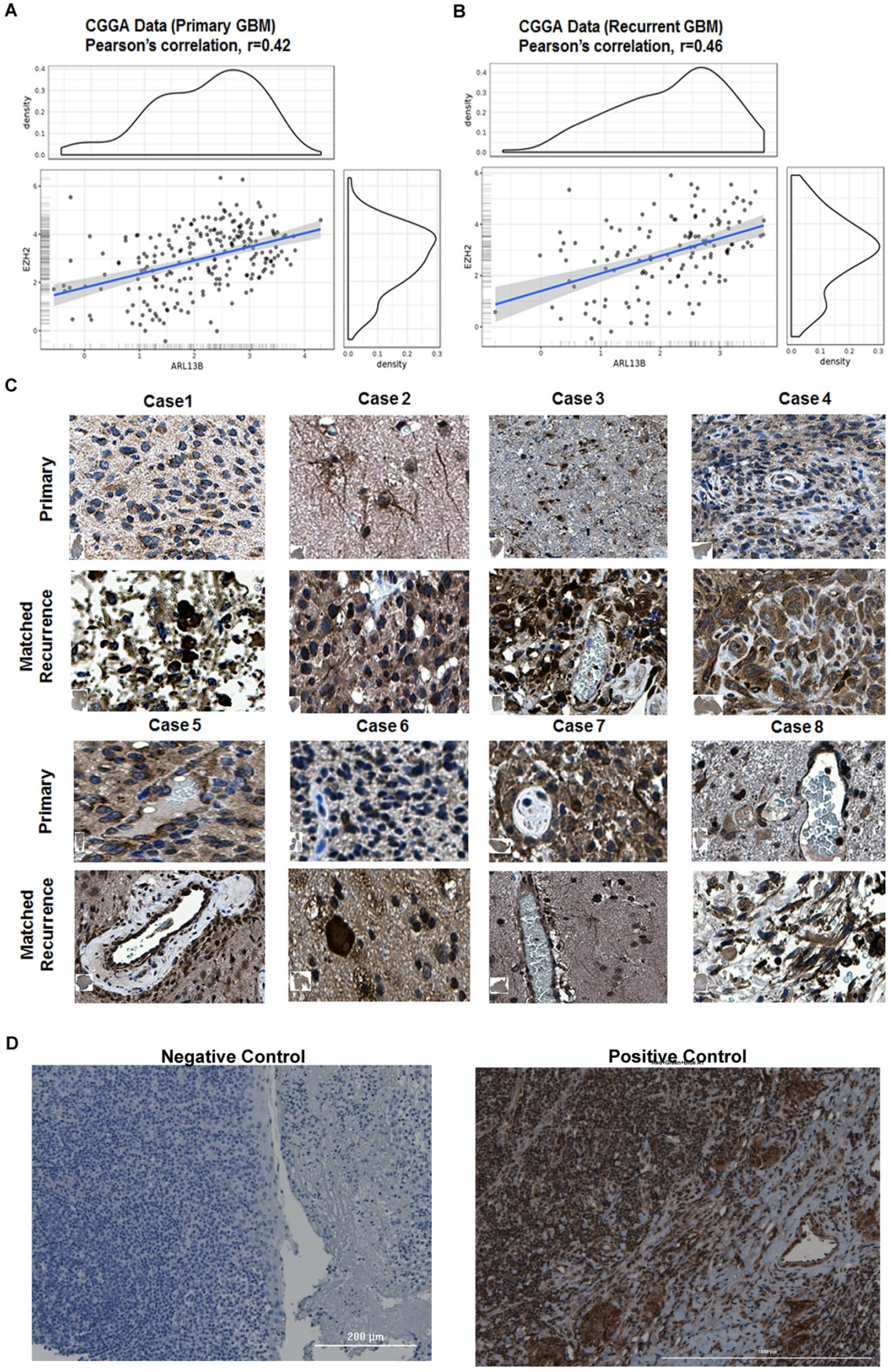

Supplementary Figure 6

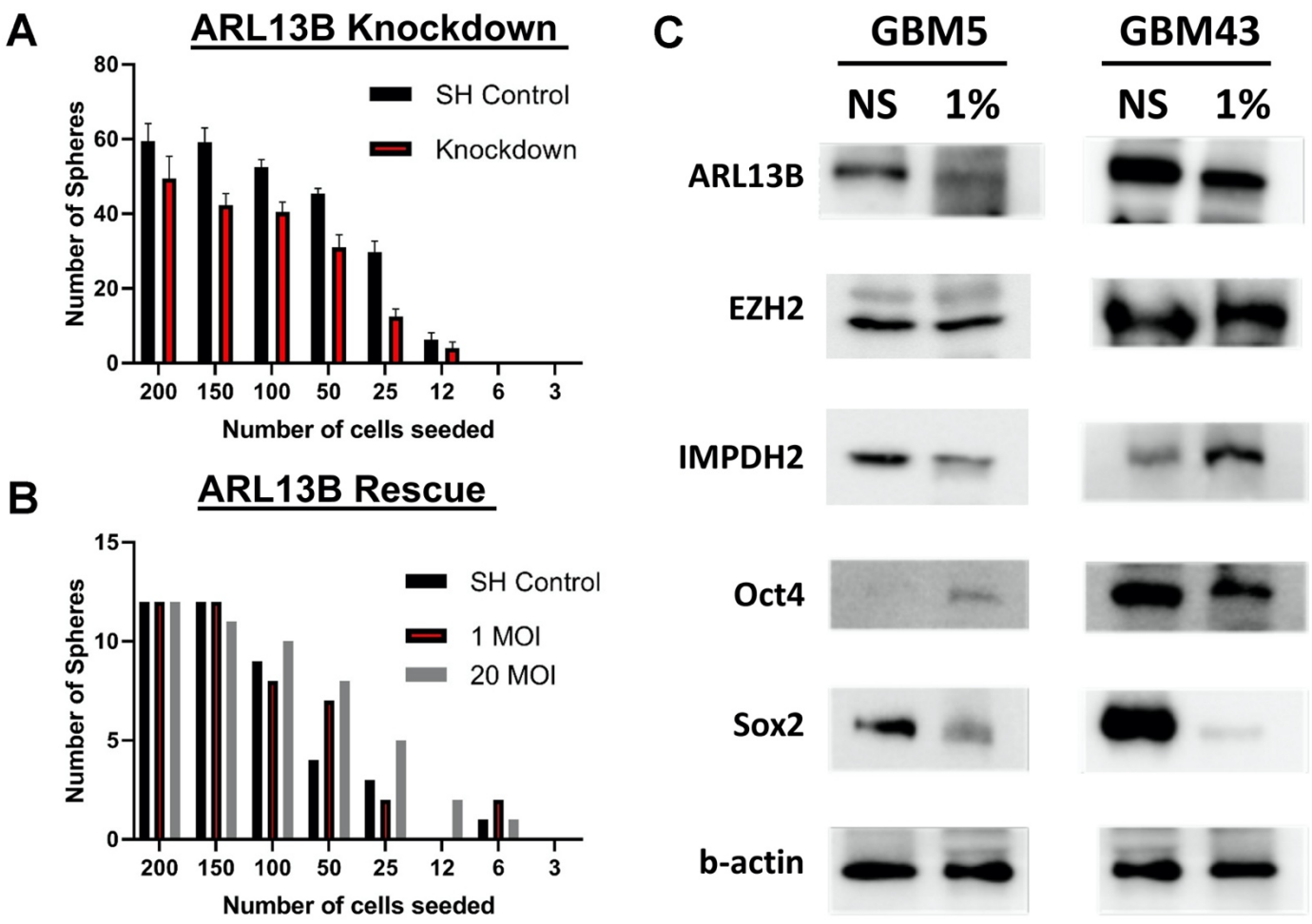

Supplementary Figure 7

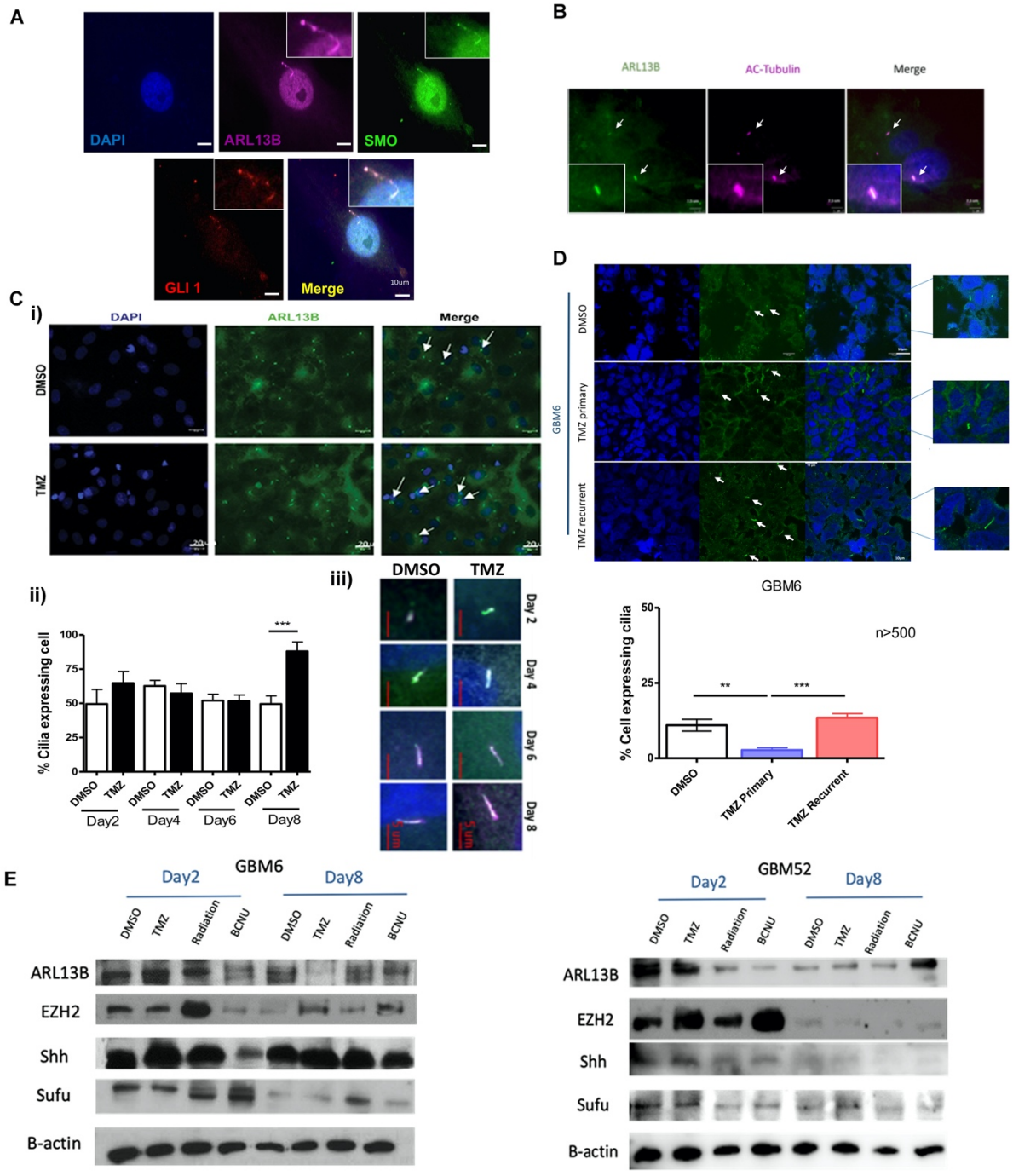

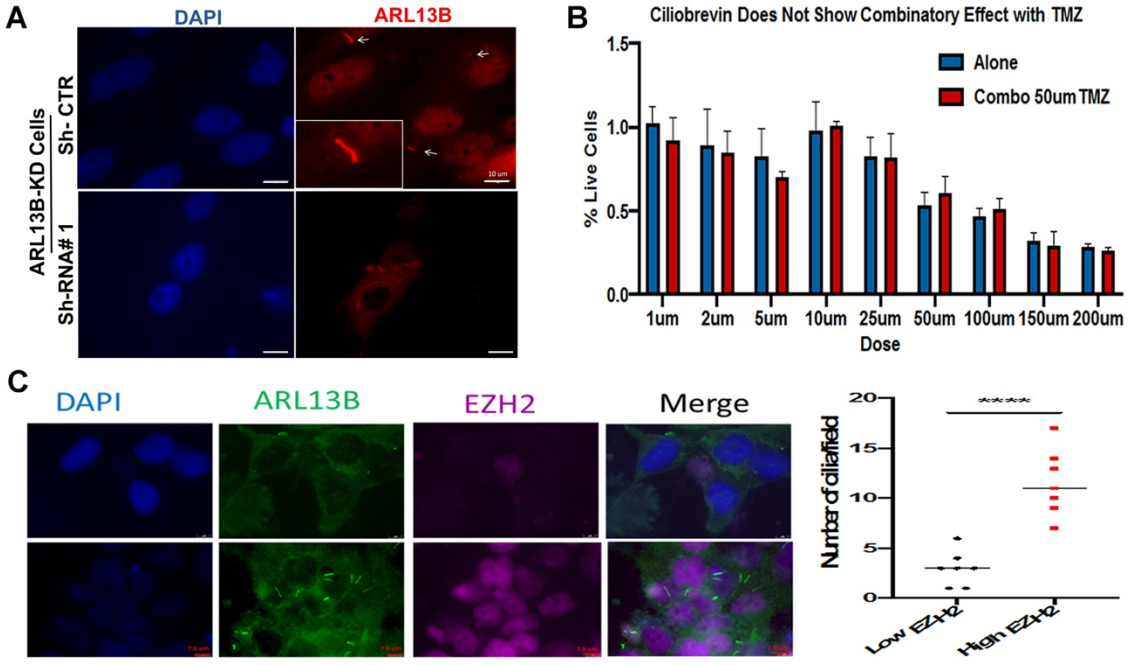
A
DAPI
ARL13B
ARL13B-KD Cells
Sh- CTR
Sh-RNA# 1
B
Ciliobrevin Does Not Show Combinatory Effect with TMZ
Alone
Combo 50um TMZ
% Live Cells
1.5
1.0
0.5
0.0
1um
2um
5um
10um
25um
50um
100um
150um
200um
Dose
C
DAPI
ARL13B
EZH2
Merge
Number of ciliated cells
20
15
10
5
0
Low EZH2
High EZH2

Supplementary Figure 9

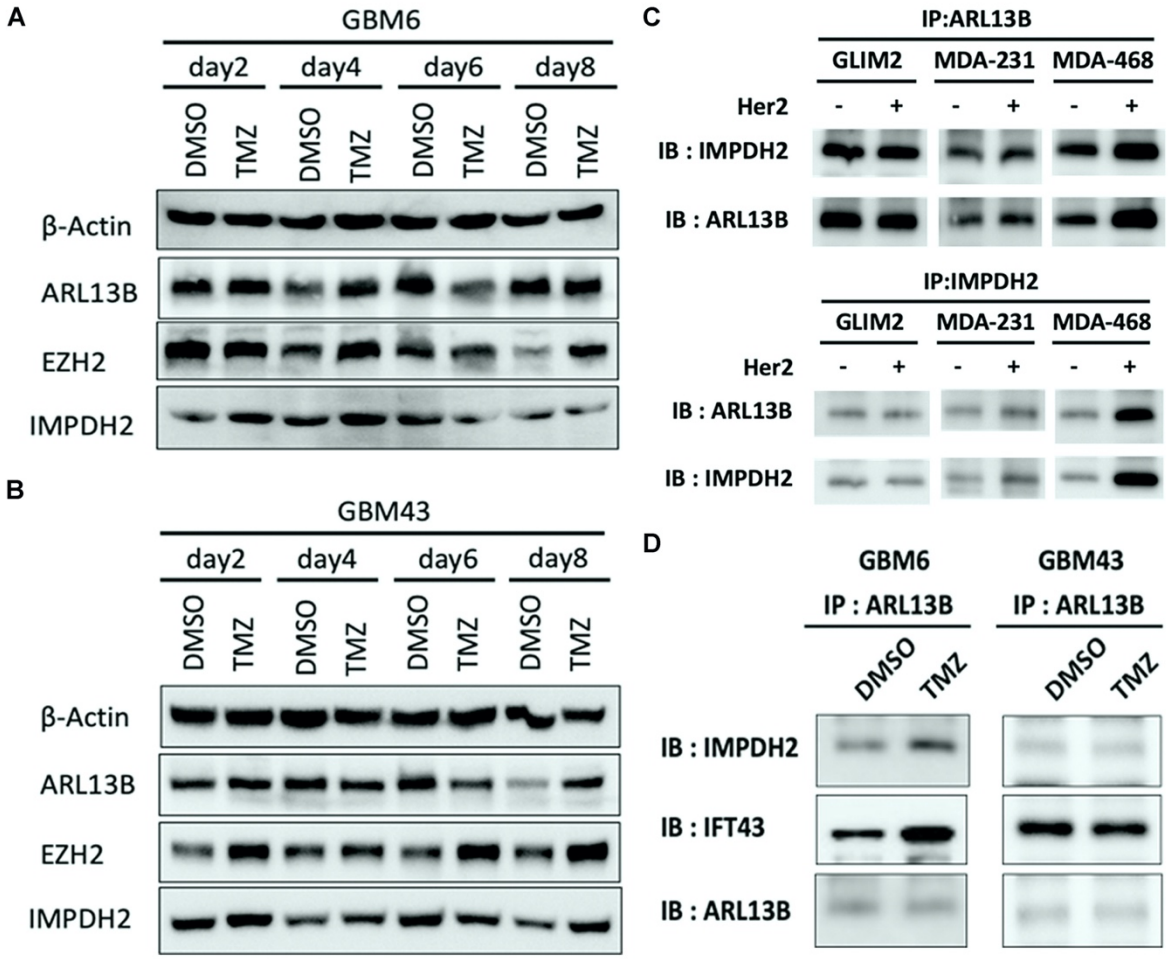

Supplementary Figure 10

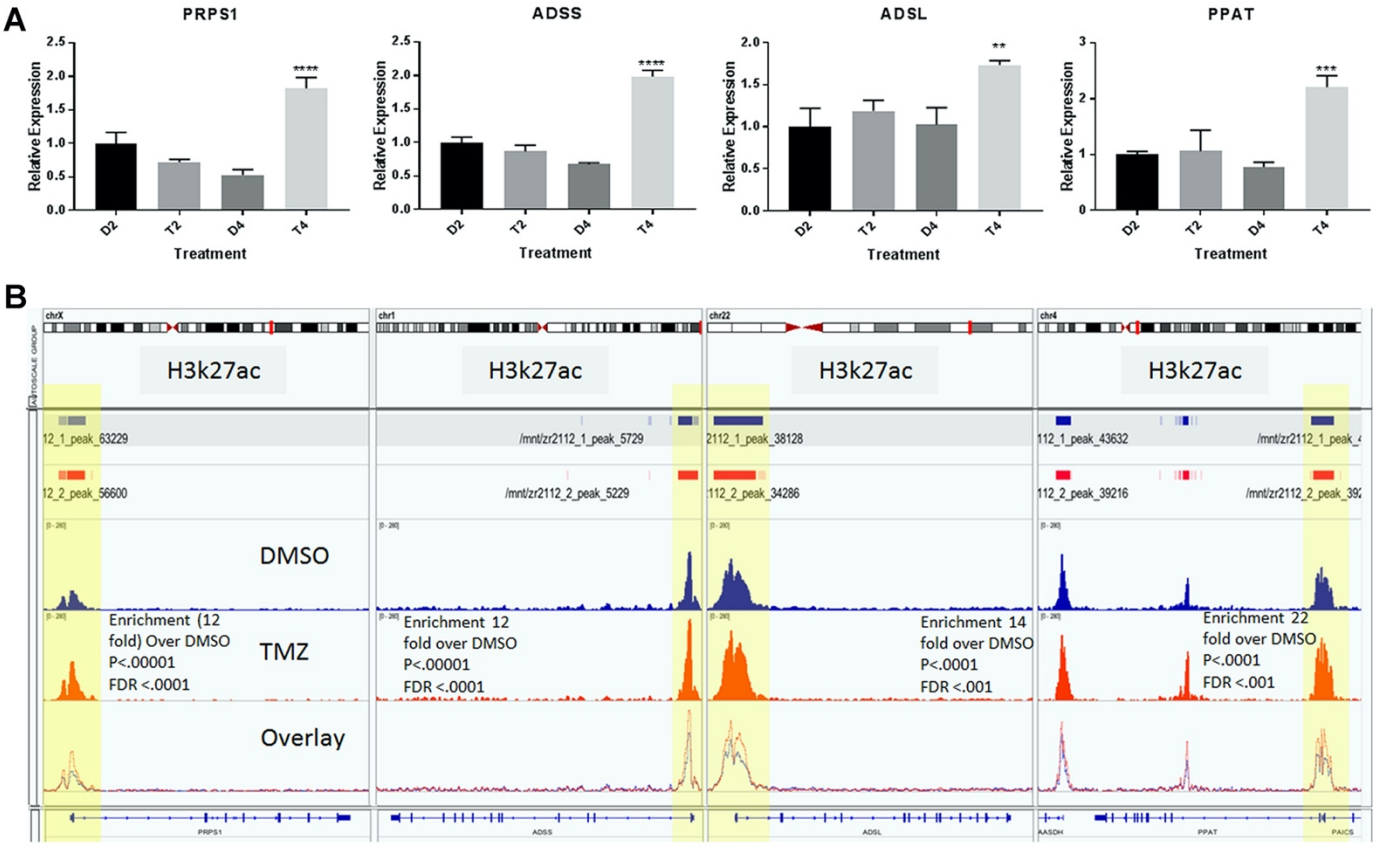

Supplementary Figure 11

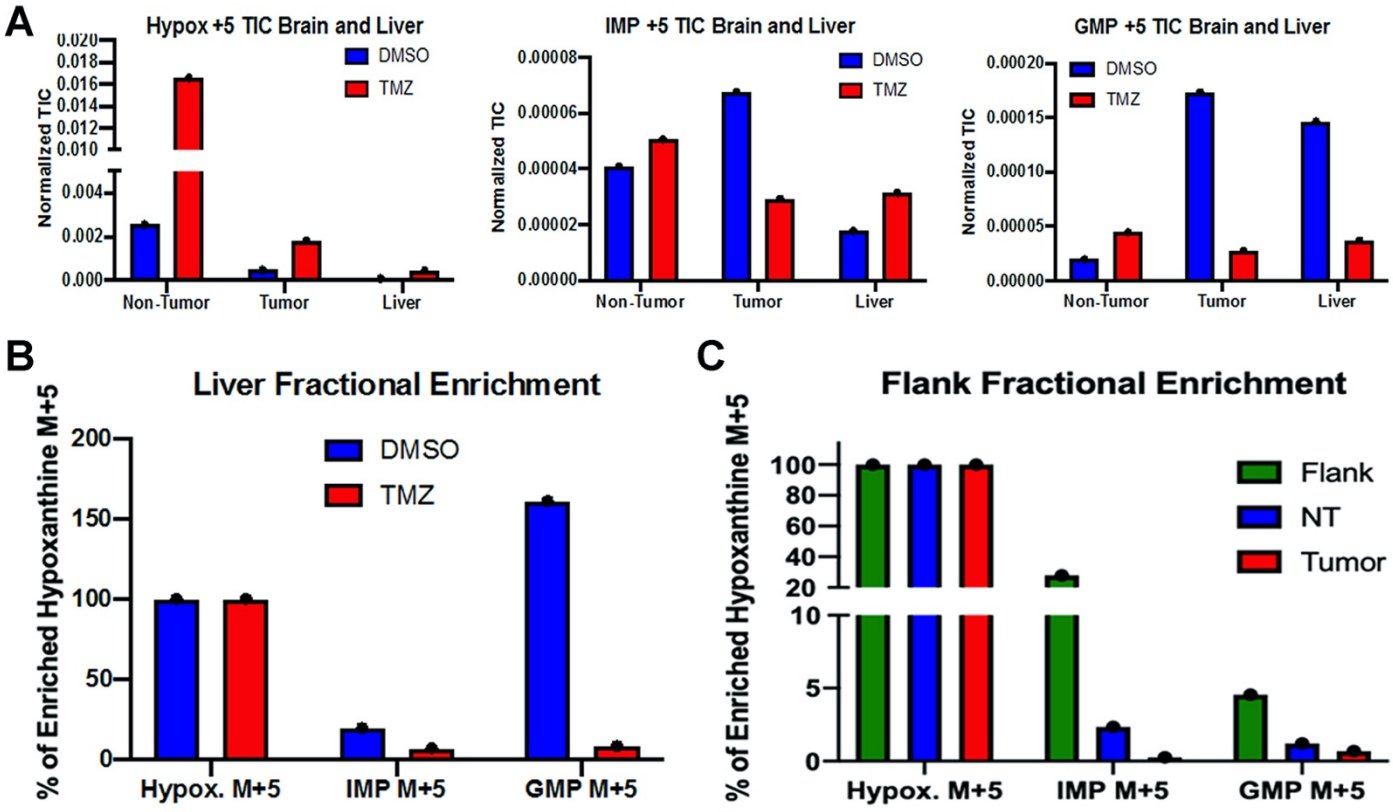

Supplementary Figure 12

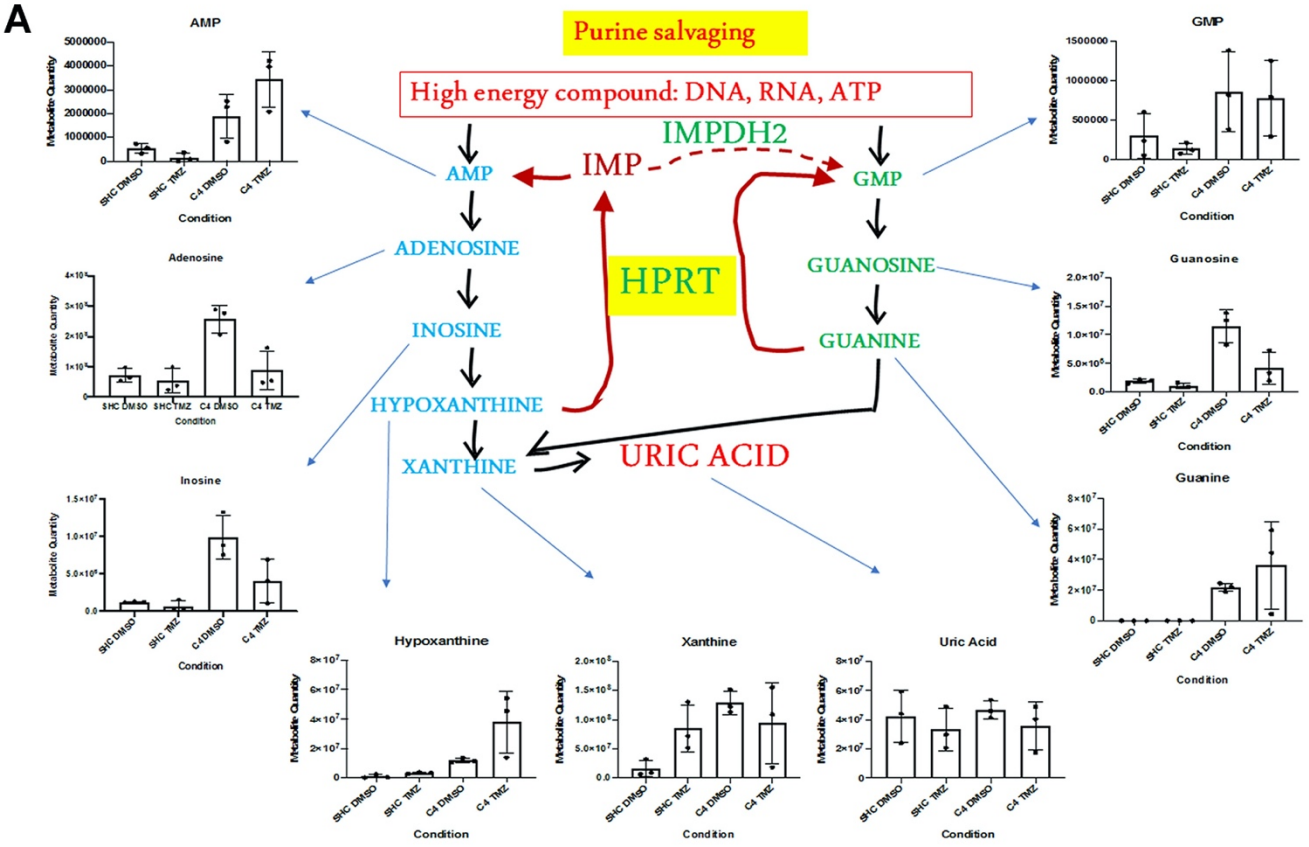

Supplementary Figure 13

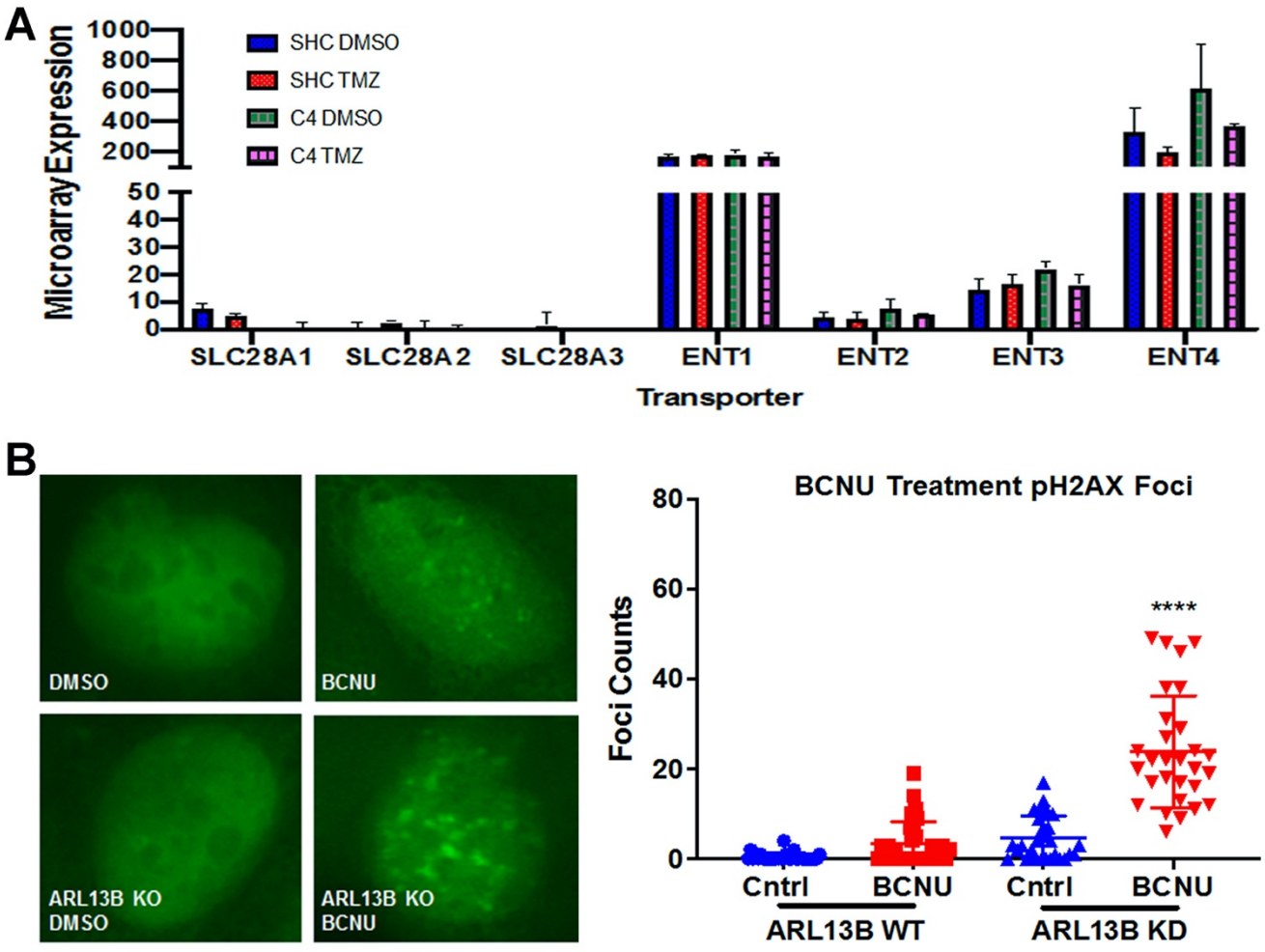

Supplementay Figure 14

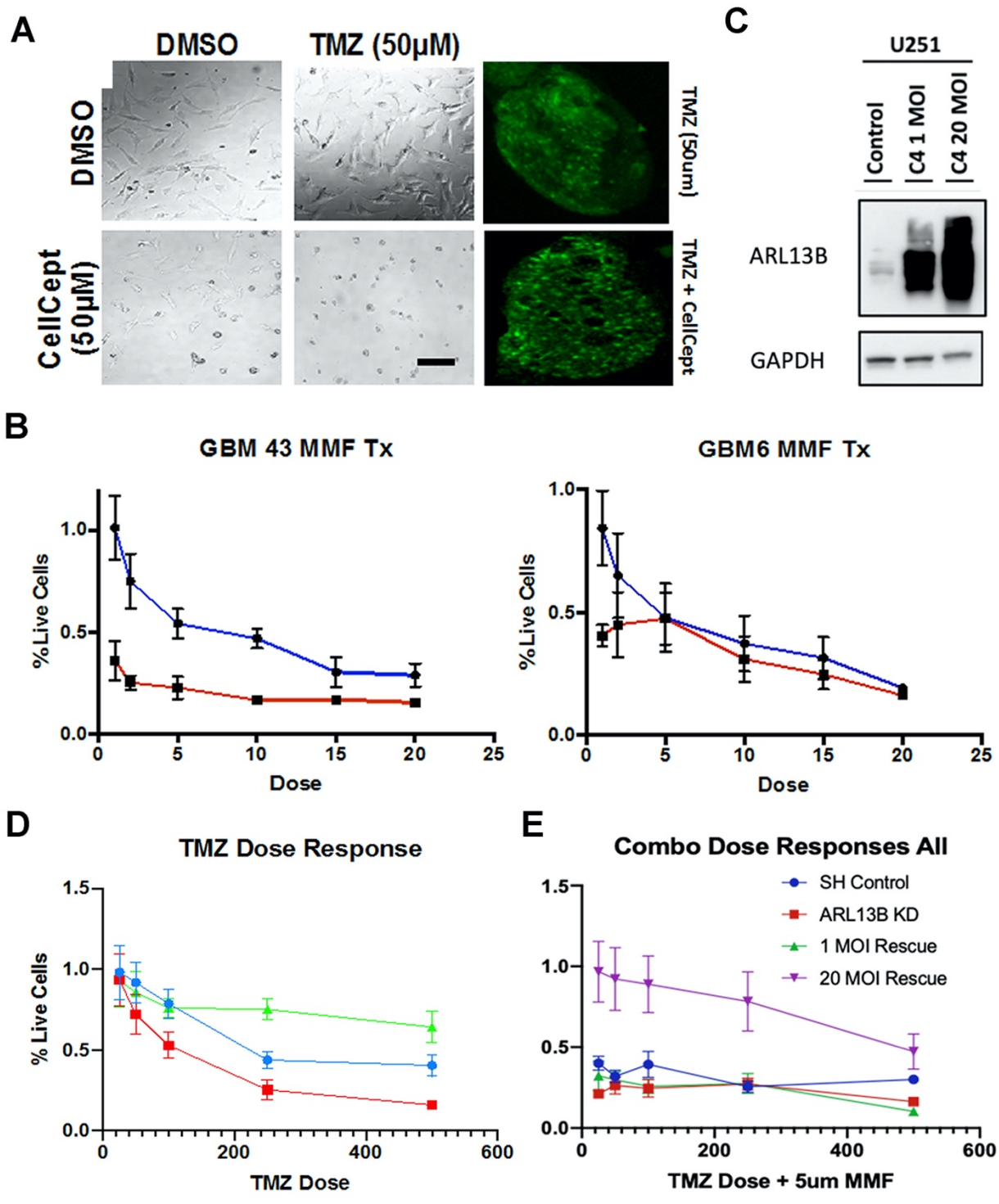

Supplementary Figure 15

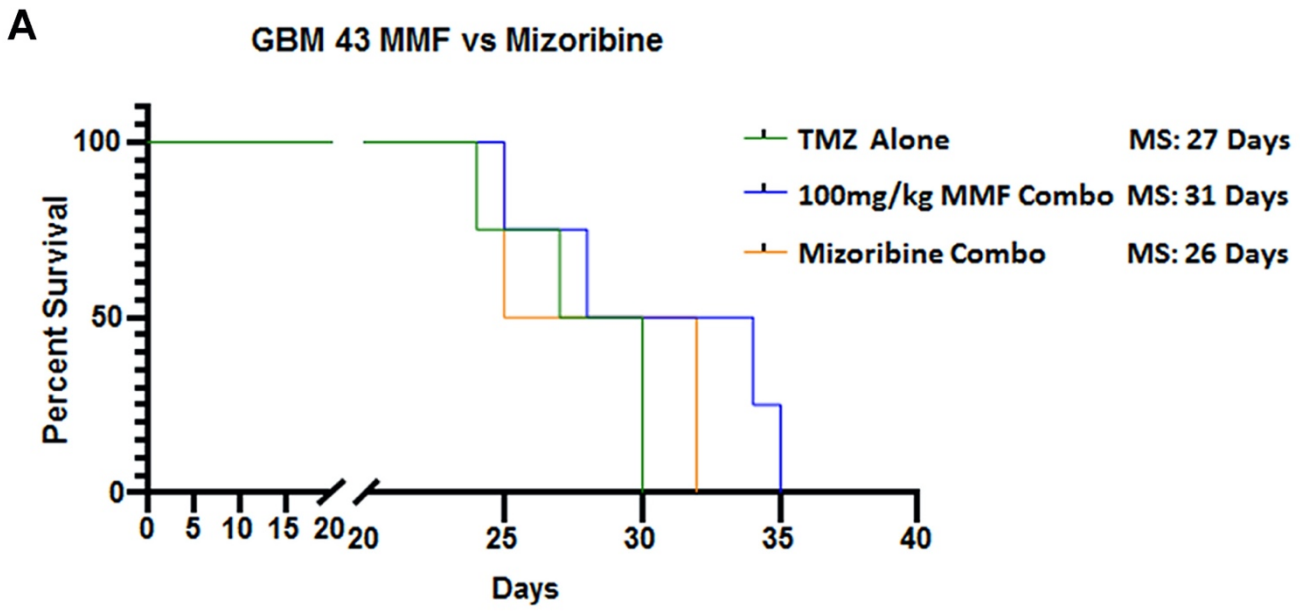

Supplementary Figure 16

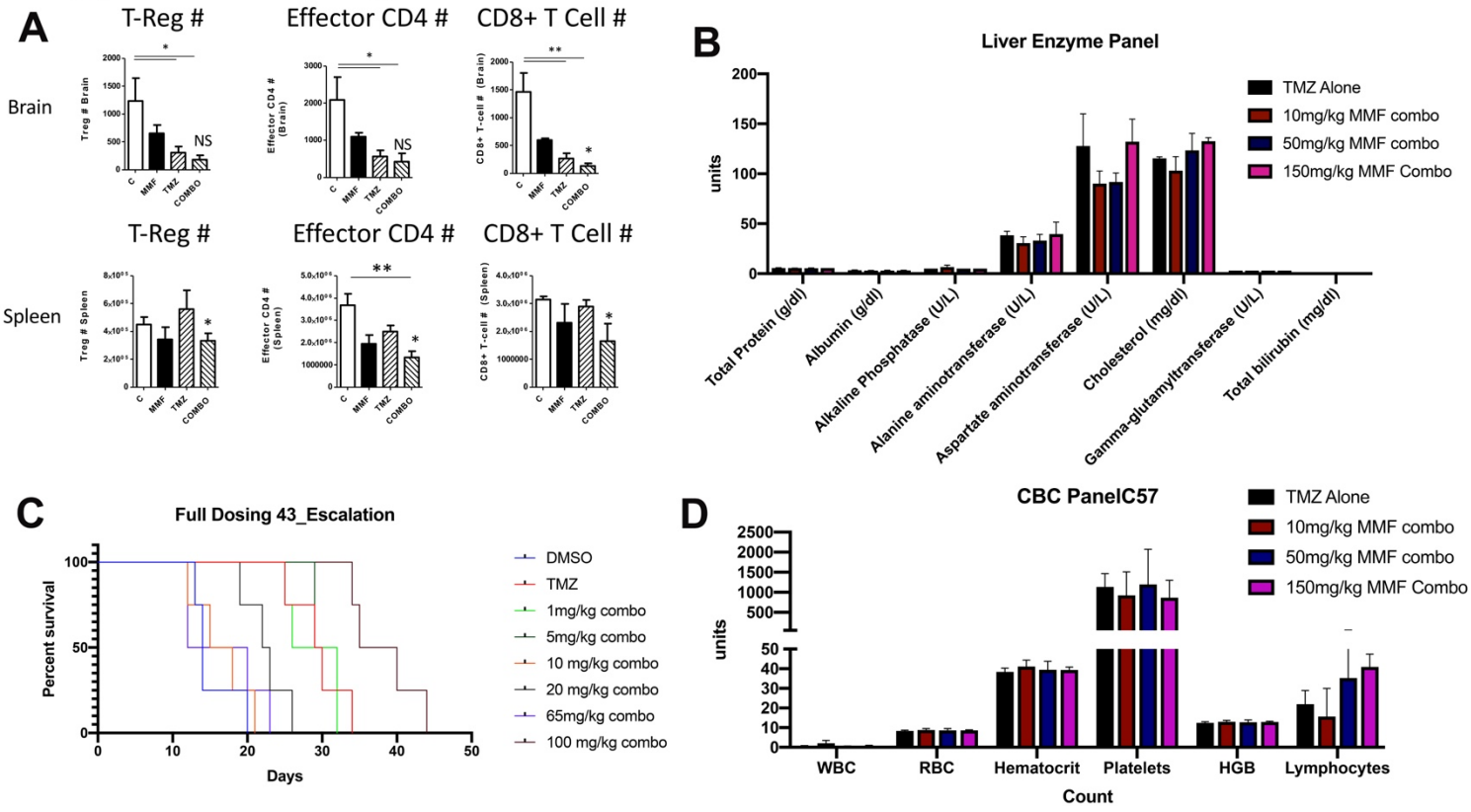

Uncropped Immunoblot gel:

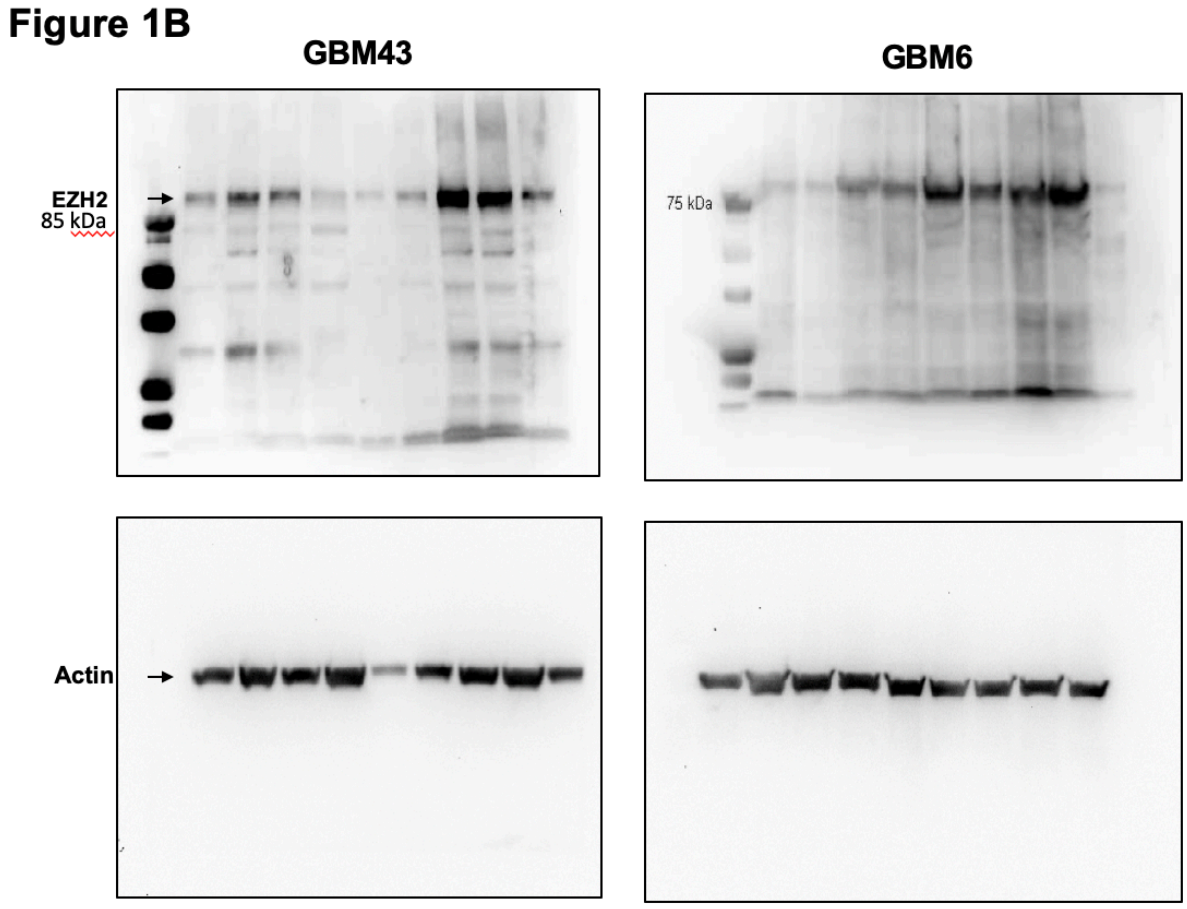

Figure 2D

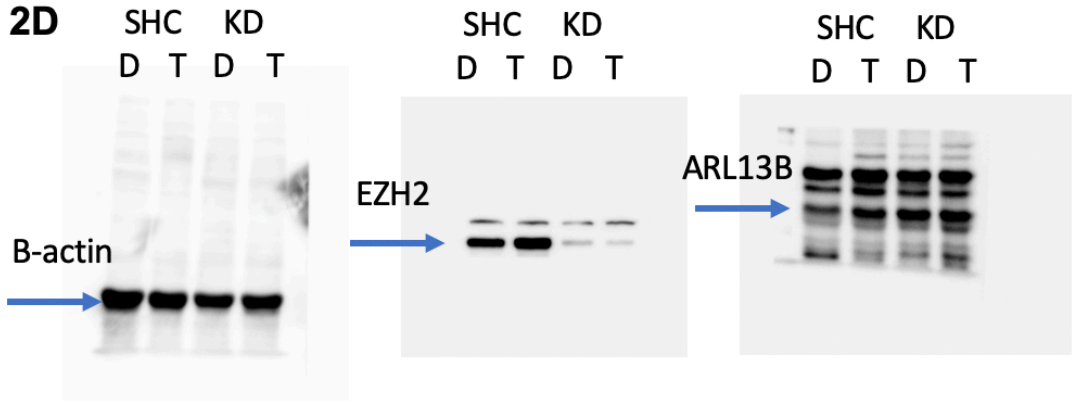

Figure 3 Panel C and Supp. Figure 5

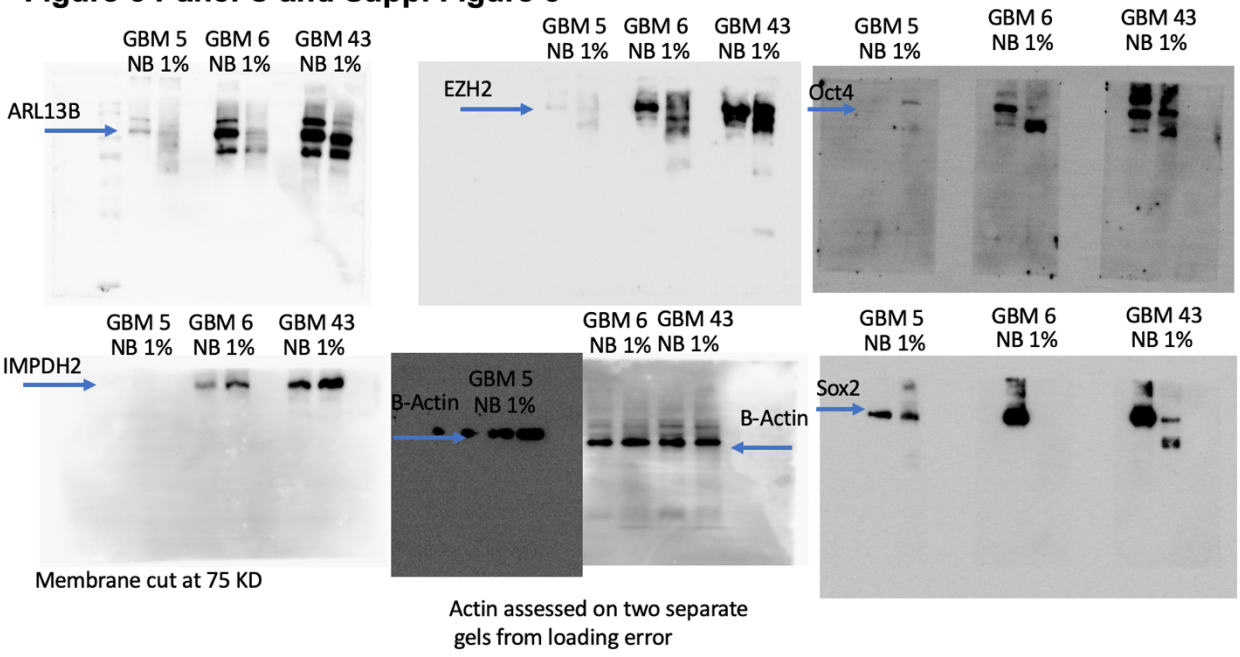

Figure 4E (Top)

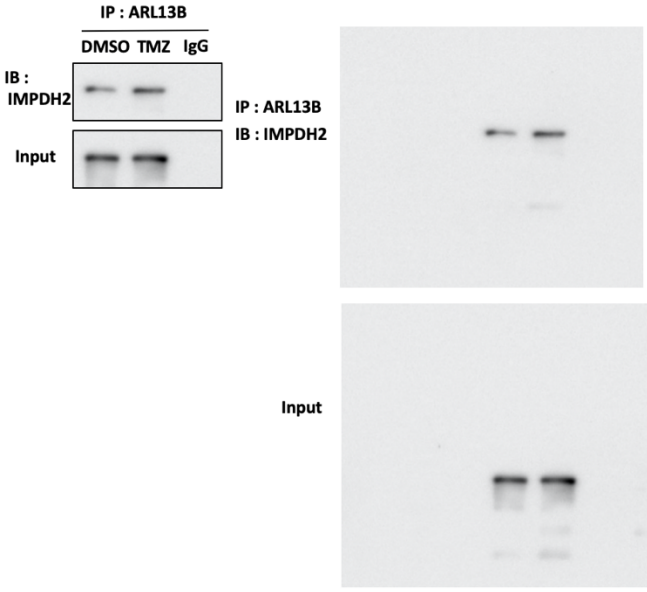

Figure 4E (Bottom)

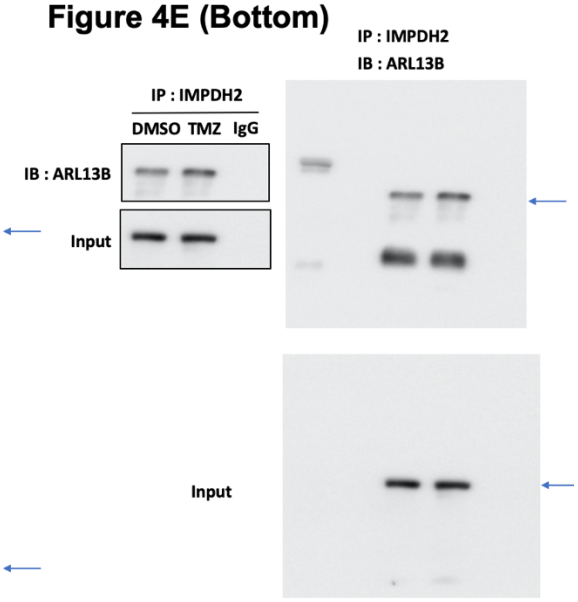

Figure 4G (Left)

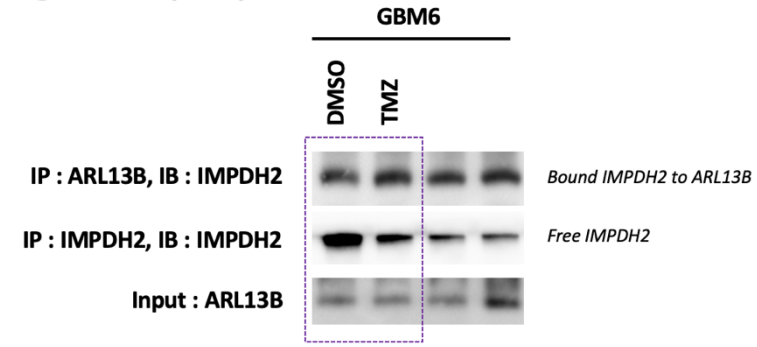

IP : ARL13B, IB : IMPDH2 (left 2 lanes)

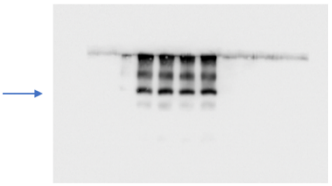

IP : IMPDH2, IB : IMPDH2 (left 2 lanes)

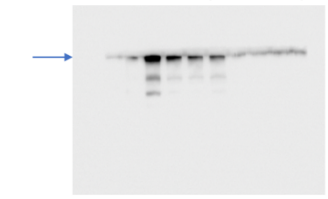

Input : ARL13B (left 2 lanes)

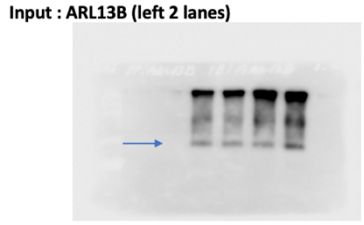

Figure 4G (Right)

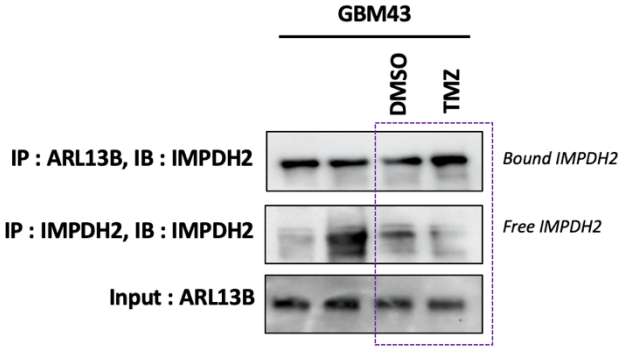

IP : ARL13B, IB : IMPDH2
Right two lanes

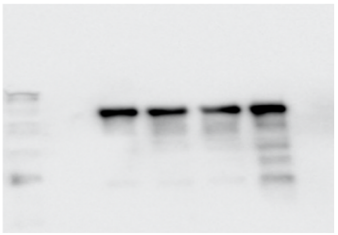

IP : IMPDH2, IB : IMPDH2
Right two lanes

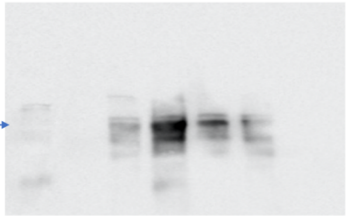

Input : ARL13B
Right two lanes

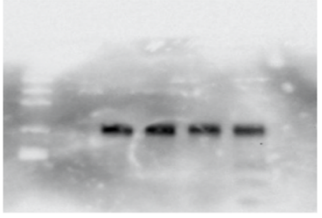

Figure 6C

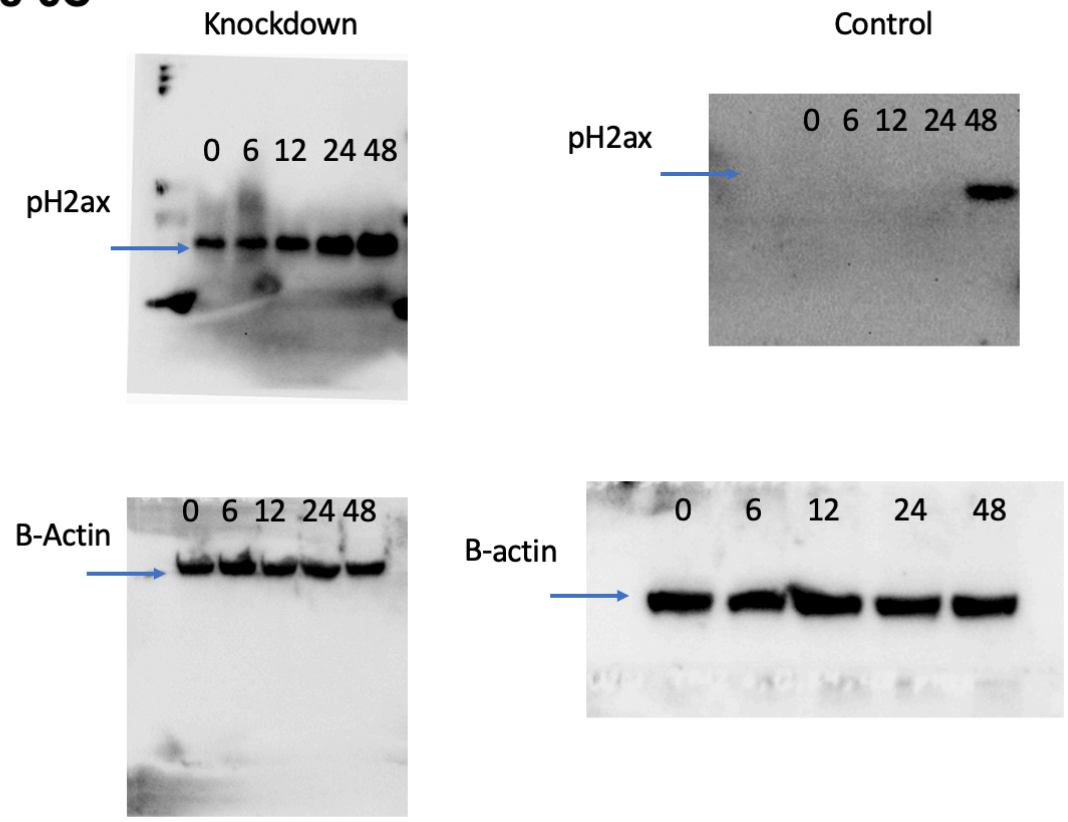
Knockdown
Control
pH2ax
0 6 12 24 48
pH2ax
0 6 12 24 48
B-Actin
0 6 12 24 48
B-actin
0 6 12 24 48

Sup Fig 3

GBM 43

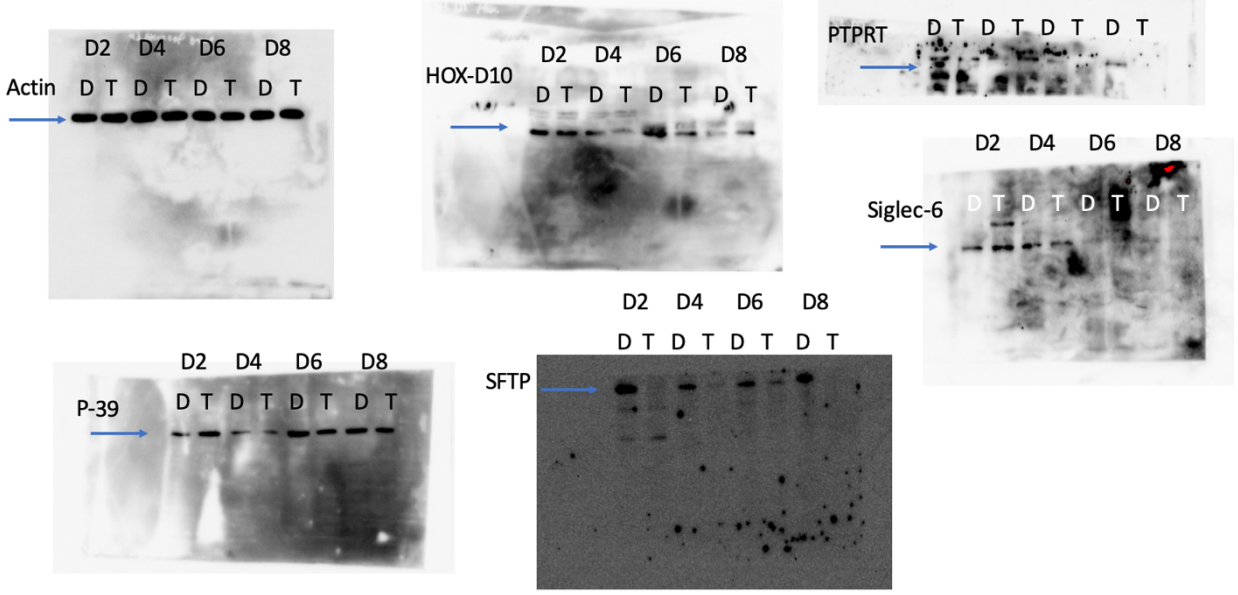

Sup Fig 3

GBM 5

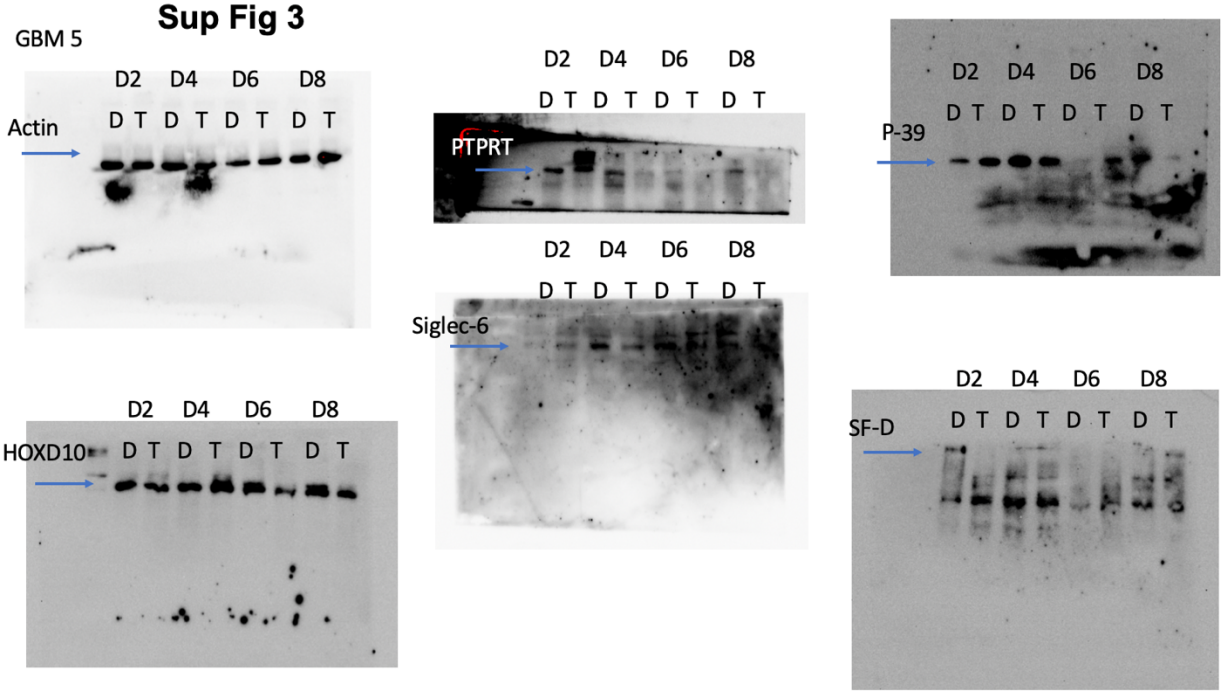

Sup Fig 6

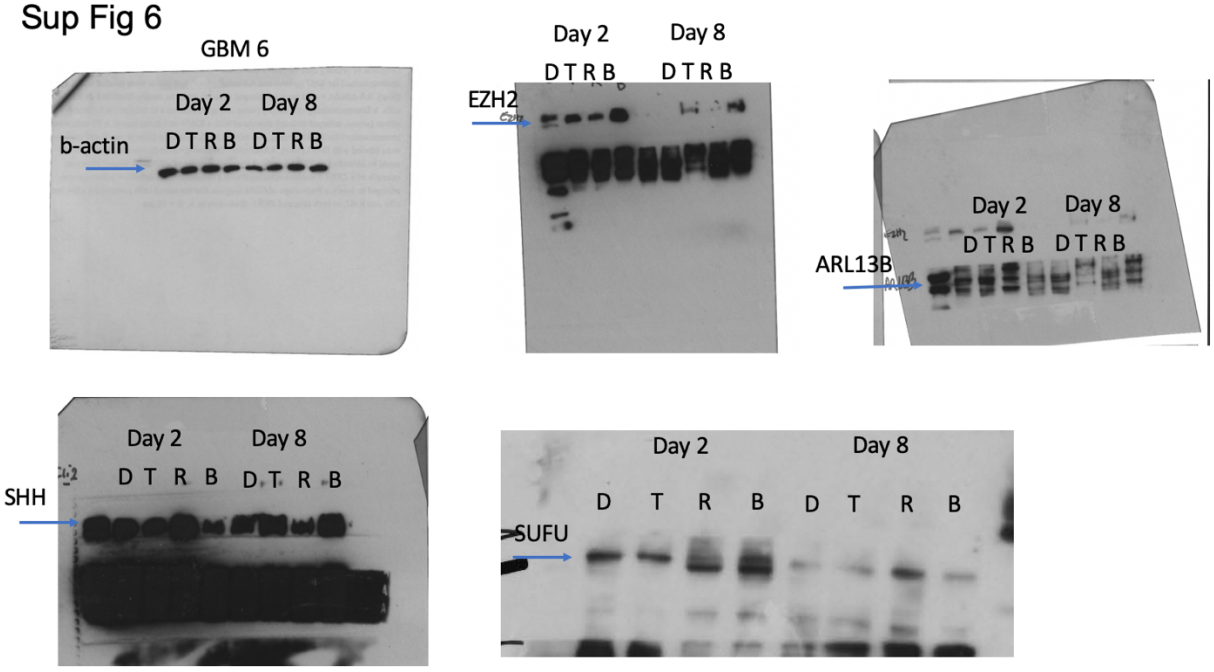
GBM 6
Day 2
Day 8
b-actin
D T R B D T R B
Day 2
Day 8
D T R B D T R B
EZH2
Day 2
Day 8
D T R B D T R B
ARL13B
Day 2
Day 8
D T R B D T R B
SHH
Day 2
Day 8
D T R B D T R B
SUFU

Sup Fig 6 GBM 52

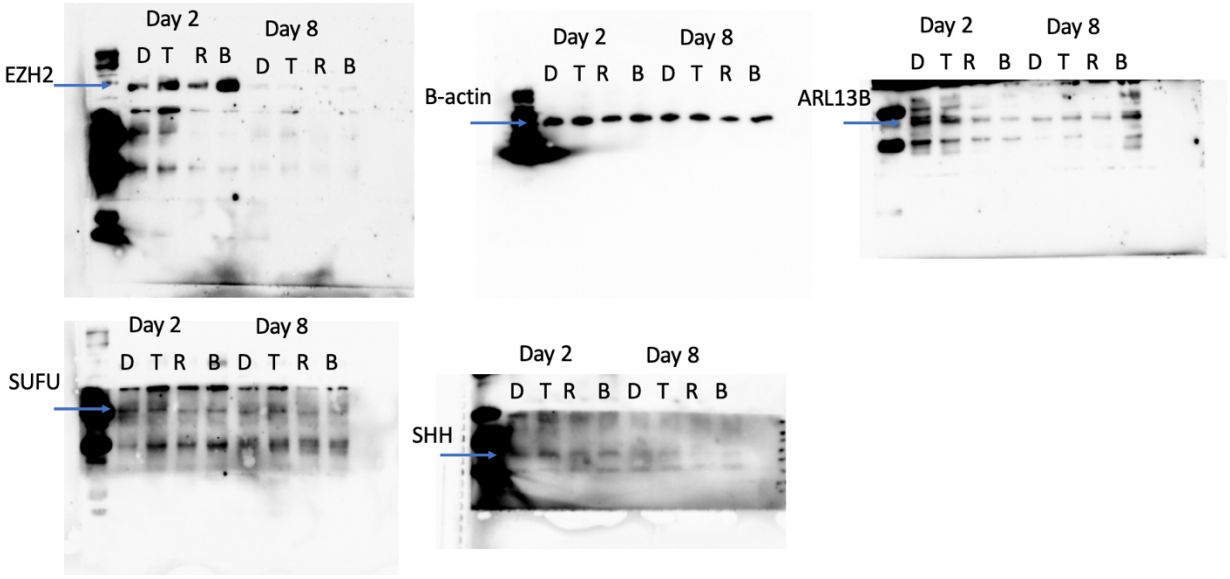

Sup fig 8

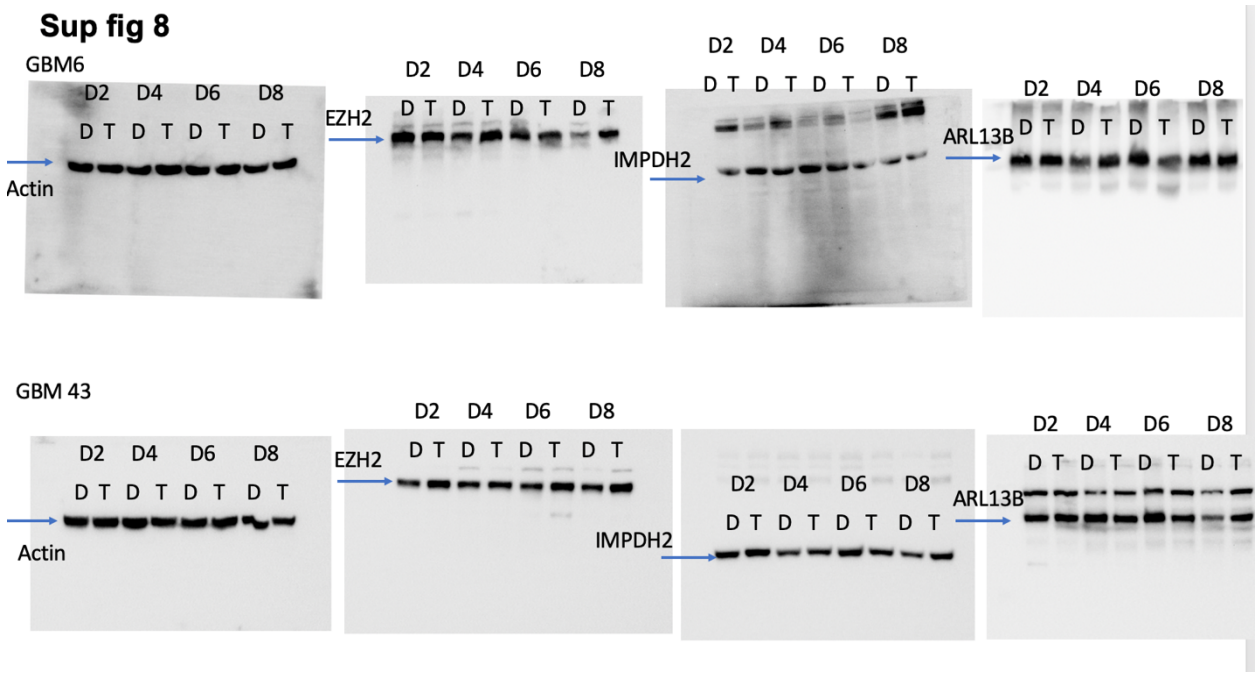
GBM6
D2 D4 D6 D8
D T D T D T D T
Actin
EZH2
IMPDH2
ARL13B
GBM 43
Actin
EZH2
IMPDH2
ARL13B

Supplementary 8C

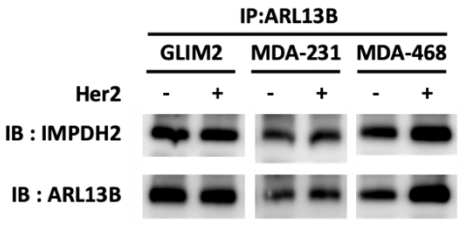

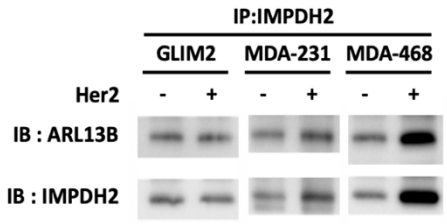

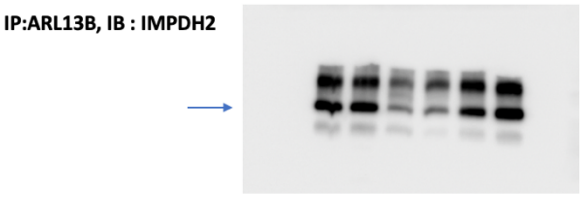

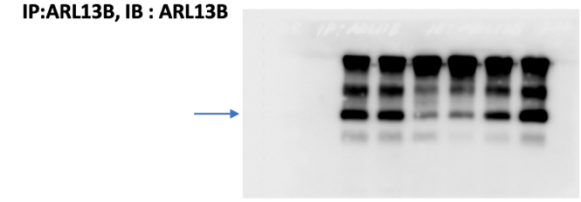

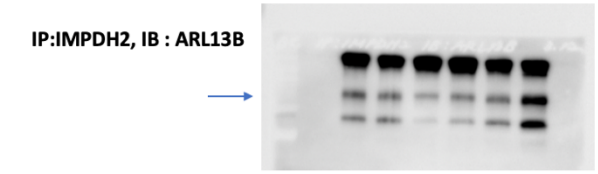

Supplementary 8D

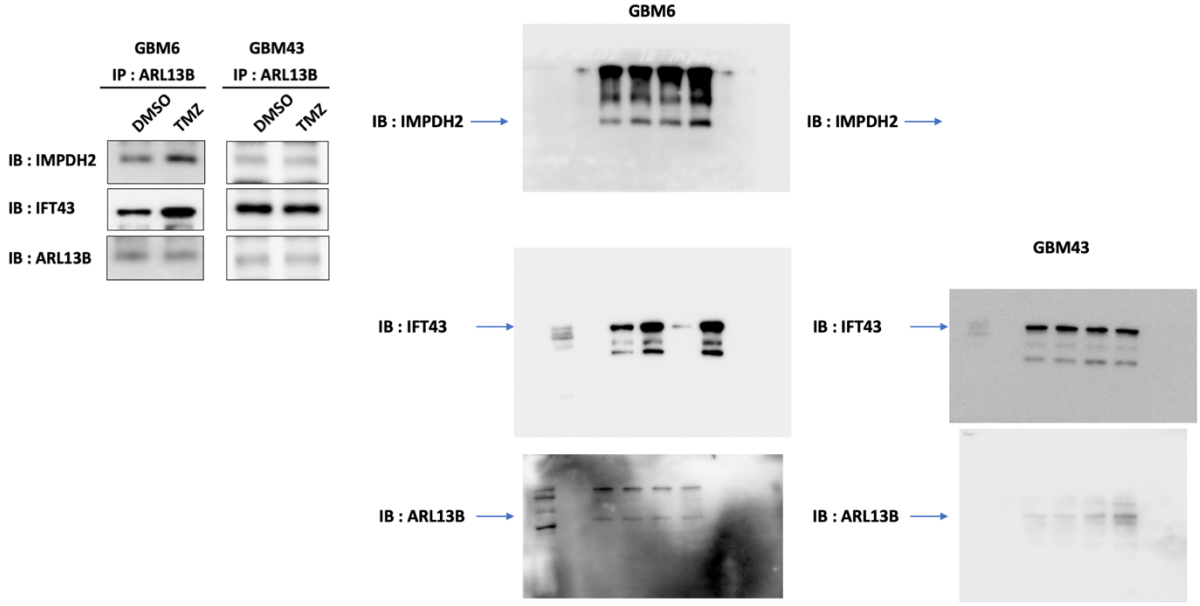

Supplementary 14C